ENGINEERING JOURNAL

Article

Towards 5G Cellular: Understanding 3D In-Building Single Band and Multi-band Small Cells with Control /User-plane Coupled and Separation Architectures with a Novel Resource Reuse Approach

Rony Kumer Saha[1,a*], **Yan Zhao**[2,b], **and Chaodit Aswakul**[1,c]

1 Wireless Network and Future Internet Research Group, Department of Electrical Engineering, Faculty of Engineering, Chulalongkorn University, Bangkok 10330, Thailand
2 International School of Engineering, Faculty of Engineering, Chulalongkorn University, Bangkok 10330, Thailand
E-mail: [a]rony107976@gmail.com (Corresponding author), [b]yan.z@chula.ac.th, [c]chaodit.a@chula.ac.th

Abstract. In this paper, we present numerous small cell base station, i.e. femtocell base station (FCBS), with control-/user-plane coupled and separation architectures based on the number of transceivers and operating frequency bands to serve control-/user-plane traffic. A single transceiver enabled FCBS can operate at either a co-channel microwave of the overlaid macrocell or a millimeter wave band. For multiple transceivers, dual transceivers are considered operating at both bands. FCBSs are deployed in a number of buildings with each floor modeled as 5×5 square-grid apartments. The co-channel interference with FCBSs is avoided using enhanced intercell interference coordination techniques. We propose a static frequency reuse approach and develop an algorithm by avoiding adjacent channel interferences from reusing frequencies in FCBSs. We also develop a resource scheduling algorithm for FCBSs with CUCA and CUSA to evaluate system level performances with a multi-tier network. It is found that a single transceiver co-channel microwave enabled FCBS with CUCA provides the worse, whereas a single or dual transceivers millimeter wave enabled FCBS with CUSA provides the best overall system capacity and FCBSs' energy efficiency performances. Besides, we show the outperformances of the proposed resource reuse approach over an existing approach in literature in terms of system capacity and fairness among FCBSs with CUCA. Finally, we point out the applicability of a multi-band enabled FCBS and several features and issues of FCBSs with CUCA and CUSA.

Keywords: 5G, architecture, femtocell, frequency band, in-building, control-/user-plane, resource reuse.

ENGINEERING JOURNAL Volume 21 Issue 3
Received 27 February 2017
Accepted 25 April 2017
Published 15 June 2017
Online at http://www.engj.org/
DOI:10.4186/ej.2017.21.3.309

DOI:10.4186/ej.2017.21.3.309

1. Introduction

1.1. Background

The envisaged high capacity demand of next generation, i.e. fifth generation (5G), mobile networks is expected to be driven mainly by three major techniques, namely small cell network densification, spectrum extension, and spectral efficiency technique [1]. The architecture of small cell base stations (SCBSs), i.e. femtocell base stations (FCBSs), for serving control-plane and user-plane (C-/U-plane) data traffic particularly in indoor environments, plays a significant role on how effectively these three major enabling techniques as aforementioned can be applied to achieve the required capacity demand of 5G networks. In existing heterogeneous networks (HetNets), a common feature is tightly coupled control-plane (C-plane) and user-plane (U-plane) irrespective of the degree of density and heterogeneity, which is one of the major reasons for most problems that the network densification is facing, e.g. low energy efficiency, complex interference management, higher signaling overhead and backhaul network requirement, and clumsy mobility management. As the mobile data traffic demand increases, existing networks have been facing problems from providing the necessary capacity that causes to initiate network architectural design innovations.

To address such a high capacity requirement, though small cells (SCs) are deployed in the coverage of macrocells (MCs), the tight coupling of C-/U-plane in conventional network architectures, which is also termed as C-/U-plane coupled architecture (CUCA), restricts the flexibility in network operation and performance management. This is because, even though there is no data traffic demand from user equipments (UEs), such tight coupling of C-/U-plane causes to switch the transmit power of a base station (BS) always on in order to ensure a ubiquitous coverage and hence results in a poor resource utilization and unnecessary energy consumption, leading to a low energy efficiency performance [2]. These call for developing a new architecture where C-/U-plane are decoupled to serve high data rate services, to switch the transmit power of a SCBS on and off based on the actual data traffic demand, and to ensure an always-on connectivity. Such a network architecture is termed as C-/U-plane separation architecture (CUSA) [2-3] and is considered as one of the major changes in 5G networks [4]. In CUSA, the C-plane is served by MCs operating typically at a low frequency such as below 3 GHz to provide large cell coverages, and the U-plane is served by SCs, e.g. femtocells (FCs), operating typically at a high frequency such as millimeter wave (mmWave) to provide high data rate services to UEs as shown in Fig. 1.

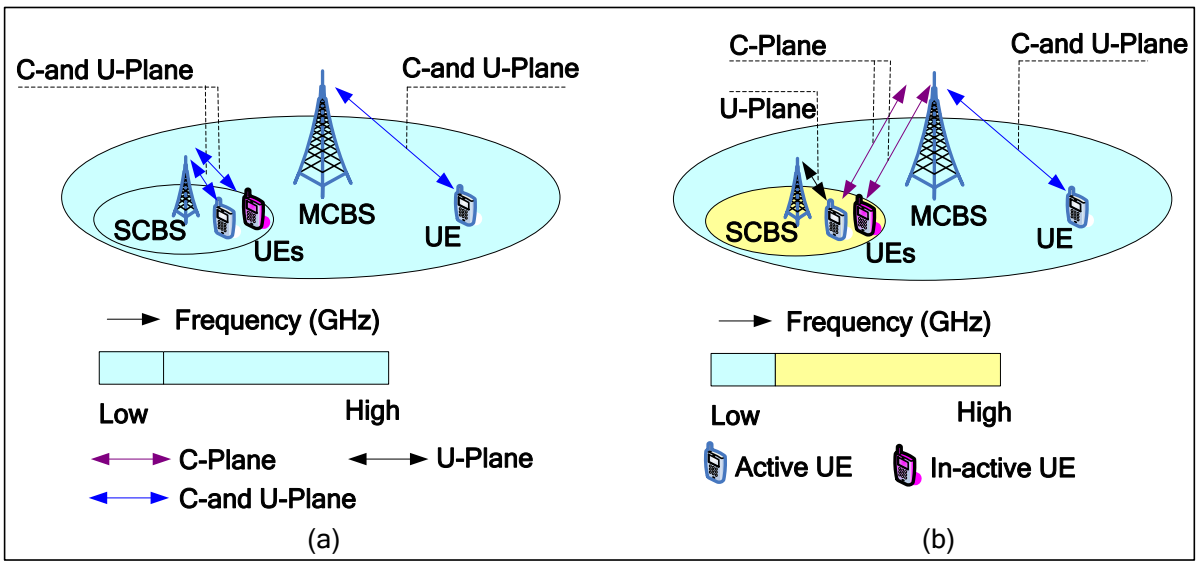

Fig. 1. CUCA and CUSA [2].

Moreover, as another major technique, increasing the system bandwidth to address such a high capacity demand of 5G, the co-existence of a number of frequency bands with diverse propagation characteristics (e.g., microwave and mmWave bands) within the same system is expected in 5G networks [5]. Besides, traffic is generated non-uniformly network wide, and the characteristics of traffic generated by C-/U-plane

are asymmetric. Hence, these high capacity, non-uniform, and asymmetric traffic has a direct impact on the capability of a SCBS resulting the requirement of an adaptive SCBS, and one way to address this feature is to implement more than one transceivers in a SCBS operating at dual bands with diverse propagation characteristics, e.g. microwave and mmWave bands. Having a SCBS operated at dual bands, based on traffic characteristics, each SCBS can switch to mmWave band during a high traffic demand and to microwave band during a low traffic demand. Further, because of small traffic volume, C-plane traffic can be served at the microwave frequency, whereas large traffic volume of U-plane can be served at the mmWave frequency.

However, because of the scarcity of bandwidth availability in microwave bands and an additional cost from licensing a new high frequency band, the third major technique as aforementioned, i.e., spectral efficiency improvement technique, such as reusing the same microwave and mmWave spectrums in SCBSs has been seen as one of the effective ways to address the high capacity demand of 5G. Since most data traffic is generated in indoor environments, e.g. dense urban multi-storage buildings, the co-channel interference (CCI) associated with reusing the same spectrum of any bands in FCBSs within a building more than once is one of the major challenges to overcome, and an appropriate clustering of FCBSs in a building can be an effective way to address such CCI in order to reuse resources in FCBSs at an optimal distance satisfying certain constraints, e.g. per link quality limit [6].

1.2. Related Work

An extensive level of researches is ongoing, particularly on CUSA [2-3], [7-9] as one of the major enablers to achieve high indoor capacity. Authors in [2-3], [7-8] proposed to split C-/U-plane by using different BSs where C-plane is served by the macrocell base station (MCBS) operating typically at a low microwave frequency, and U-plane is served by SCBSs, i.e. FCBSs. Each FCBS is enabled with a single transceiver operating at a high frequency mmWave band, and hence the dual connectivity feature of a UE to communicate with two nodes operating at different frequencies was proposed in [10]. A similar SCBS architecture was also proposed by the authors in [1]. Recently, the authors in [9] proposed to address C-/U-plane splitting by implementing dual transceivers at the same FCBS where one of the transceivers operates at the co-channel microwave frequency as that of the MCBS and the other at the mmWave frequency. They showed that splitting with the same FCBS outperforms splitting via different BSs in terms of, e.g. energy efficiency, system capacity, and spectral efficiency.

Further, a considerable amount of researches on numerous issues of FC, e.g. [11-14] for the interference management and resource reuse and allocation in FC networks, [15-16] for enforcing a minimum distance between FCBSs, and [17-22] for FC clustering and resource allocation have been addressed. Mathematical tools such as stochastic geometric approaches [15-16] have been applied under 2-dimensional (2D) random BS location scenario to address issues such as interference modeling and enforcement of a minimum distance between BSs. However, such approaches are mostly limited to a simple homogenous Poisson point process or Matern hardcore process and an amorphous shape of cell areas.

A number of studies also addressed issues of clustering and resource reuse in FCs under 3-dimensional (3D) in-building scenarios. Authors in [23] proposed a graph based adaptive FC clustering scheme for inter-FC interference coordination within the same building. In [24], authors proposed an adaptive soft frequency reuse scheme where groups of FCs are formed using the received signal strength indication from UEs, and different frequency reuse factors and transmission powers are adjusted to mitigate mutual interference. Authors in [25] exploited fractional frequency reuse using iBuildNet to propose a cooperative transmission and a semi-static interference mitigation scheme for in-building dense FCs. Also, authors in [17] proposed a dynamic clustering based cognitive sub-band allocation scheme to reduce inter-FC interference. FC clusters (FCLs) are formed using inter-FC interference graphs, and resources are reused in each disjoint FCL within a building. Authors in [26] proposed an analytical model using planar-Wyner model for intra-floor and linear-Wyner model for inter-floor interference modeling in a building to derive a minimum distance between co-channel FCBSs for a number of optimization constraints in order to reuse microwave frequencies in FCBSs with CUCA deployed in the building. They also proposed and analyzed the performance of a resource reuse approach where a fraction of the system bandwidth is kept reserved for reusing in each co-channel FCBS (cFCBS) such that a cluster is formed with respect to each cFCBS. The remaining resource block (RB) resources of the system bandwidth are allocated to all non-cFCBSs in the building to show that the spectral efficiency of 5G networks can be achieved. However, the proposed

resource reuse approach is susceptible to a change in the number of reused RBs per cFCBS for the fairness in resource allocation among all FCBSs in a building since RB resources are considered reusing only in cFCBSs.

Although several issues of FCBSs have already been addressed as aforesaid, other than that in [26], an approach for reusing the system bandwidth in FCBSs deployed in more realistic 3D multi-storage buildings is not obvious. In addition, though a number of architectures of FCBSs for serving C-/U-plane traffic have been proposed in existing literatures, to the best of our knowledge, a common understanding on how these FCBS architectures perform, and a performance evaluation of these architectures for C-/U-plane traffic capacity and energy efficiency has not been addressed yet by any existing contributions, which can help network operators and vendors give insights on considering an appropriate FCBS architecture for 5G networks. In this paper, we aim at addressing the aforementioned issues.

1.3. Consideration and Contribution

We consider a multi-tier network consisting a MC, a number of outdoor picocells (PCs) and indoor FCs deployed in multi-storage buildings. Each building consists of a number of floors with 5×5 square-grid apartments, which is compliant with the 3rd Generation Partnership Project (3GPP) urban dense 5×5 square grid based FC model for Long-Term Evolution-Advanced (LTE-Advanced) system evaluation [27]. Each apartment has one FCBS. Both the MCBS and all picocell base stations (PCBSs) are operated at the microwave band. The whole microwave bandwidth is reused in FCBSs within a building, and the cross-tier CCI between macro UEs (MUs) and femto UEs (FUs) is avoided using the almost blank subframe (ABS) based enhanced intercell interference coordination (eICIC) technique. However, the mmWave band is used only in FCBSs. The clustering of FCBSs is done by adopting the analytical model proposed in [26].

We first present various SCBS architectures for serving C-/U-plane traffic based on the number of transceivers and their operating frequency bands existing in a SCBS, namely a single transceiver operating either at a co-channel microwave or an mmWave band and dual transceivers operating at both the co-channel microwave and mmWave bands. We propose a static frequency resource reuse and allocation approach and develop an algorithm to reuse resources in FCBSs. With a system level simulation, we evaluate first the performances of a number of C-/U-plane coupled and separation FCBS architectures in terms of the system capacity and energy efficiency. For a given link quality constraint between a FCBS and a UE and the number of FCBSs in a building, we demonstrate the outperformance of our proposed resource reuse approach for FCBSs with CUCA in terms of the overall system capacity and fairness in resource allocations in FCBSs over the proposed resource reuse approach in [26].

The paper is organized as follows. In section 2, numerous FCBSs with C/U-plane coupled and separation architectures are discussed. Section 3 discusses FC networks, interference management, and region of exclusion (RoE) modeling to reuse resources in FCBSs in any buildings. The FC clustering technique and proposed resource reuse approach and algorithm for FCBSs are covered in section 4. A multi-tier system architecture and interference management for CUCA and CUSA are discussed in section 5. Section 6 covers the problem formulation, including multi-tier network model, capacity and energy efficiency formulations for numerous FCBS architectures, proportional fair scheduling, and Jain's fairness index. A resource scheduling algorithm for system level performance evaluations along with the resource scheduler implementations are discussed in section 7. In section 8, simulation parameters and assumptions are given, performance evaluations of various FCBS architectures are carried out, and performance comparisons of the proposed resource reuse approach with that proposed in an existing research work are performed. A number of key features and issues of a FCBS with CUCA and CUSA and the applicability of a multi-band enabled FCBS in terms of non-uniform traffic and split architectures are pointed out in section 9. We conclude the paper in section 10. A list for the abbreviations and selected notations used in this paper are given in Table 1 and Table 2, respectively.

2. Femtocell Base Station Architectures and Resource Allocations

Based on the number of transceivers and their operating frequencies considered in a FCBS to route C-/U-plane traffic, a number of FCBSs both with CUCA and CUSA can be developed as explained in the following. In CUCA, a MCBS typically operates at a low microwave frequency. However, FCBSs can be operated at either the same microwave frequency as that of the MCBS with a proper cross-tier CCI management between the macro-tier and the femto-tier (Fig. 2(a)) or a different frequency (Fig. 2(b)) from

that of the MCBS at the cost of licensing an additional frequency band. Both BSs serve C-/U-plane traffic to their respective UEs.

Table 1. A list of abbreviations.

Abbreviation	Full Form
2D	2-Dimensional
3D	3-Dimensional
3GPP	Third Generation Partnership Project
5G	Fifth Generation
ABS	Almost Blank Subframe
APP	ABS Pattern Period
BS	Base Station
C-/U-plane	Control-Plane and User-Plane
CCI	Co-Channel Interference
cFCBS	Co-Channel Femtocell Base Station
CH	Cluster Head
C-plane	Control-Plane
CSG	Closed Subscriber Group
CUCA	Control-Plane and User-Plane Coupled Architecture
CUSA	Control-Plane and User-Plane Separation Architecture
dB	Decibel
dBi	Decibel Relative to an Isotropic Radiator
dBm	Decibel-Milliwatts
DL	Downlink
eICIC	Enhanced Inter-Cell Interference Coordination
E-UTRA	Evolved Universal Terrestrial Radio Access
FCBS	Femtocell Base Station
FU	Femto User Equipment
HetNets	Heterogeneous Networks
LTE-Advanced	Long Term Evolution-Advanced
MCBS	Macrocell Base Station
mmWave	Millimeter Wave
MU	Macro User Equipment
PC	Picocell
PCBS	Picocell Base Station
RB	Resource Block
RoE	Region of Exclusion
SC	Small Cell
sFCBS	Serving Femtocell Base Station
sFU	Serving Femto User Equipment
TTI	Transmission Time Interval
UE	User Equipment
UL	Uplink
UL/DL	Uplink and Downlink
U-plane	User-Plane

In CUSA, splitting of C-/U-plane can be obtained by implementing either a single or multiple transceivers at a FCBS described as follows. In a single transceiver implemented FCBS, C-/U-plane can be decoupled by operating the FCBS either at the co-channel frequency as (Fig. 2(c)) or at a different frequency from that of its overlaid MCBS (Fig. 2(d)). Unlike CUCA, C-plane traffic of all UEs is served only by the MCBS, and U-plane traffic of FUs is served by FCBSs. However, like CUCA, when operating at the co-channel microwave frequency, a proper interference management between the MC-tier and FC-tier is needed in order to avoid cross-tier CCI. In contrast, there is no need for such cross-tier interference management if a FCBS is operating at a different frequency because of operating the MCBS and any FCBSs

always at orthogonal frequencies. Though it comes at the cost of licensing an additional frequency band for FCBSs, this architecture has been proposed widely in literature for 5G mobile networks [2-3].

Table 2. Selected list of notations.

Notation	Description
$d_{\min}$	Minimum distance of a cFCBS from any sFUs in intra-floor level
$d_{\text{ver,min}}$	Minimum vertical distance of a cFCBS in inter-floor level
α_{tra} and α_{ter}	Normalized intra-floor and inter-floor interference power from a cFCBS respectively
ψ_{m}	Maximum number of cFCBSs per tier in both intra-floor and inter-floor levels
$\alpha_{\text{c,tra}}\left(d_{\text{tra}}\right)$ and $\alpha_{\text{c,ter}}\left(d_{\text{ter}}\right)$	CCI power (dBm) at a sFU from a cFCBS at d_{tra} and d_{ter} respectively
$\alpha_{\text{tra}}\left(d_{\text{tra}}\right)$	Normalized value of intra-floor interference power at an arbitrary distance d_{tra} from a cFCBS at a sFU
$\alpha_{\text{ter}}\left(d_{\text{ter}}\right)$	Normalized value of inter-floor interference power for an arbitrary distance d_{ter} at a sFU from a cFCBS located on a floor other than that of the sFCBS
d_{tra} and d_{ter}	An arbitrary distance in intra-floor and inter-floor levels between a sFU and a cFCBS respectively
d_{ver}	Vertical distance between a sFCBS and any cFCBSs on a floor other than that of the sFCBS
$\alpha_{\text{agg,tra}}$ and $\alpha_{\text{agg,ter}}$	Aggregate interference power received at a sFU from intra-floor and inter-floor cFCBSs respectively
P_{T} and $P_{\text{T,max}}$	Transmit power per FCBS and maximum transmit power of a FCBS respectively
f_{mcbs} and f_{fcbs}	Operating frequency of a MCBS and a FCBS respectively
Θ_{RoE}	Number of FCBSs per RoE in a building
$\sigma_{\text{thr,se}}$	Link spectral efficiency constraint
$\sigma_{\text{tra,se}}$ and $\sigma_{\text{ter,se}}$	Link spectral efficiencies in intra-floor and inter-floor levels respectively
$\alpha_{\text{f}}(d_{\text{ter}})$	Floor attenuation factor
M_{T} and m_{T}	Number of RBs in microwave and mmWave bandwidths respectively
ξ_{f} and ξ_{t}	Resource reuse factor and resource reuse times respectively
N and L	Number of MUs in the system and Maximum number of buildings in a MC coverage respectively
S_{F}	Number of active FCs in each building
$\boldsymbol{T}$ and $\boldsymbol{T}_{\text{ABS}}$	Simulation run time and number of ABSs in every ABS pattern period respectively
$\rho_{t,i}$	Received signal-to-interference-plus-noise ratio for a UE at RB=i in TTI=t
$\sigma_{t,i}\left(\rho_{t,i}\right)$	Link throughput at RB=i in TTI=t in bps per Hz
U_{FC}	Number of FCBSs per 3D cluster
M_{FC}	An equal number of RBs per FCBS for microwave bands per 3D cluster
m_{FC}	An equal number of RBs per FCBS for mmWave bands per 3D cluster
$\sigma_{\text{thr,cc}}$ and $\sigma_{\text{thr,df}}$	Required link spectral efficiency between a sFU and its sFCBS within a cluster for microwave and mmWave bands respectively
$\xi_{\text{t,cc}}$ and $\xi_{\text{t,df}}$	Resource reuse times for microwave and mmWave per building respectively
$\varkappa_{\text{cp}}$	Percentage of C-plane traffic for FCBSs with CUCA in both microwave and mmWave bands
η_{ee} and F_{J}	Average energy per bit transmission in J/b and Jain's fairness index respectively

In a multiple transceivers implemented FCBS, a FCBS operates at multiple frequencies. Since the number of transceivers and their operating frequencies do not vary the analysis, we consider in this paper dual transceivers at a FCBS operating at dual frequencies, namely co-channel microwave and different mmWave frequencies (Fig. 2(e)). The decoupling of C-/U-plane traffic is performed by serving traffic of each plane at different frequencies of separate transceivers. Hence, both C-/U-plane traffic of any FUs is served by its serving FCBS itself. However, when the FU is out of coverage of its serving FCBS, its C-/U-plane traffic is then served by the MCBS. Unlike the single transceiver based FCBS architecture shown in Fig. 2(d), no coordination signaling is required between the C-plane MCBS and any U-plane FCBSs. However, it comes at the cost of an additional transceiver and its operating frequency band at each FCBS as well as UE. Note that a single band option is not applicable for a multiple transceivers implemented FCBS because of considering more than one transceivers at a FCBS.

In *single band co-channel* deployment of FCBSs *with CUCA*, a certain percentage of the total number of RBs M_T in the microwave bandwidth (e.g., m_p RBs) is kept reserved to serve C-plane traffic of MUs by the MCBS in all transmission time intervals (TTIs) and C-plane traffic of FUs by the respective FCBSs by reusing m_P RBs in them following the CCI management scheme only during non-ABSs. The remaining (M_T-m_p) RBs are reused to serve U-plane traffic of FUs during non-ABSs. In contrast, for FCBSs *with CUSA* when operating at the co-channel microwave frequency, C-plane traffic of all UEs is served by the MCBS with m_p RBs, and like CUCA, (M_T-m_p) RBs are reused in FCBSs during non-ABSs. If FCBSs *with CUSA* are operating at a *different frequency*, e.g. mmWave with m_T RBs, all m_T RBs can be reused to serve U-plane traffic of FCBSs, and the MCBS serves C-plane traffic of all UEs in the system at the microwave frequency with m_p RBs. However, for FCBSs *with CUCA*, like co-channel deployment, a certain percentage of the total number of RBs m_T in the mmWave bandwidth (e.g., m_m RBs) is kept reserved and reused to serve C-plane traffic of FUs by the respective FCBSs in all TTIs. The remaining (m_T-m_m) RBs are reused to serve U-plane traffic of FUs in all TTIs.

In *multi-band* co-channel and different frequencies deployment of FCBSs *with CUSA*, (M_T-m_p) microwave RBs can be reused to serve C-plane traffic of FCBSs themselves during non-ABSs, and all m_T mmWave RBs can be used to serve U-plane traffic of FCBSs themselves in all TTIs. Unlike any single band deployments, C-plane traffic of only MUs is served by the MCBS. Note that multi-band deployment of FCBSs with CUCA is not applicable. Further, since a channel response changes with the type of frequency bands, the link quality constraints at the co-channel microwave band and different frequency mmWave band are in need of being adjusted such that the cluster sizes of FCBSs to serve both C-plane and U-plane traffic of FCBSs are the same in order to reduce computational complexity.

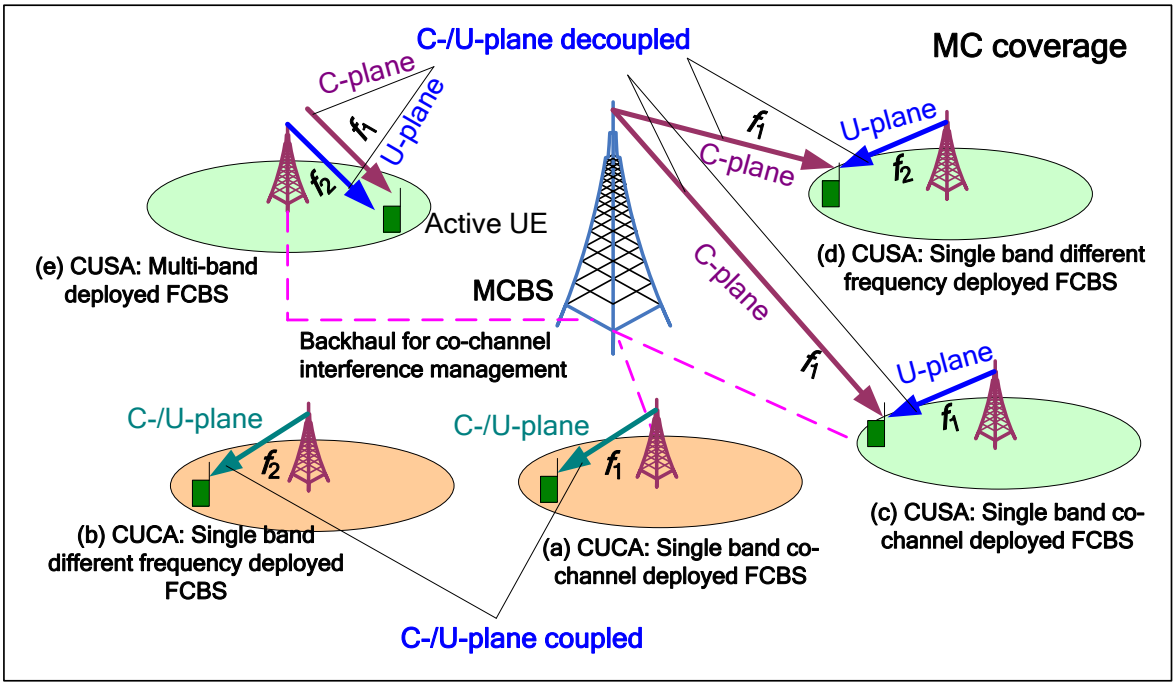

Fig. 2. FCBSs with CUCA and CUSA.

DOI:10.4186/ej.2017.21.3.309

3. In-Building Femtocell Network, Interference, and RoE Modeling

3.1. Femtocell Network Modeling

We adopt the regular grid based network and intra-and inter-floor interference modeling of FCBSs deployed in a 3D multi-floor building we proposed in [26] as follows. A 3D multi-floor building is considered consisting a number of 2D floors each with 5×5 square-grid apartments. Each apartment has one FCBS placed in the center of its ceiling. The area of each square apartment is $10\,\text{m}\times10\,\text{m}$, and a free space of 10 m is considered around each building. A FU per FCBS is considered and placed at the farthest radial distance from its serving FCBS (sFCBS). An illustration of an example aggregate interference effect of all cFCBSs at a serving FU (sFU) is shown in Fig. 3 [26]. A link between a cFCBS and a sFU is termed as CCI link, and the one between a sFU and its sFCBS is termed as desired link. For simplicity, the same CCI effect at a sFU from each cFCBS of the same tier is considered. The region up to which the aggregate interference is significant enough so that it exceeds a maximum allowable aggregate interference at a sFU is termed as the RoE for reusing the same resources of the sFCBS in any FCBSs within the RoE. Hence, a RoE in Fig. 3 is up to tier-1 and is shown in red color lines. Note that irrespective of tier indices, the maximum number of cFCBSs for a sFCBS in intra-floor level is 8. Modeling inter-floor architecture is straightforward except that an additional floor attenuation loss between a sFU and a cFCBS needs to take into account. The CCI effect from the maximum of two cFCBSs for double-sided cFCBSs and one for single-sided cFCBSs located on a vertically straight up and down floors from the serving floor of sFCBS is considered significant (Fig. 3) [26]. In [26], the modeling of intra-floor interference and inter-floor interference is carried out by using planar-Wyner model and linear-Wyner model [28] respectively. A detailed description on the FC network modelling can be found in [26].

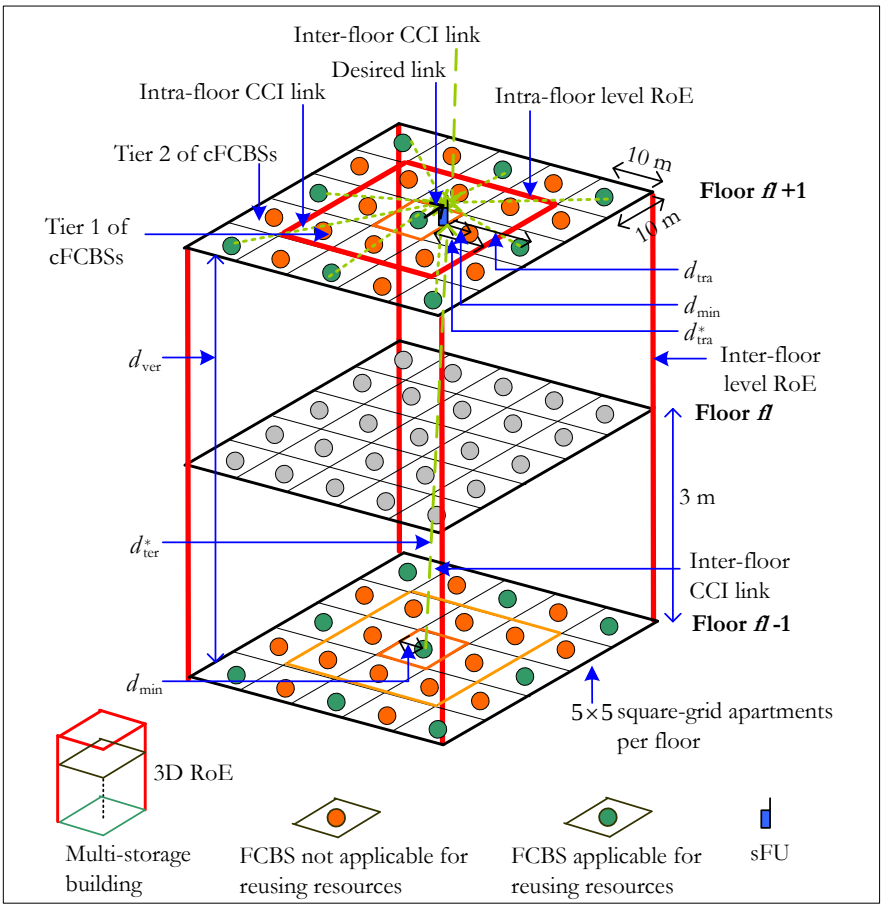

Fig. 3. Intra-and inter-floor interference modeling in a 3D regular square-grid based FC network.

3.2. Femtocell Interference and RoE Modeling

3.2.1. Interference modeling

For interference modelling in both intra-and inter-floor levels, normalization of the interference power is considered in [26] to simplify expressions. The normalized interference power is defined as the ratio of the interference power received from any cFCBSs of any tiers at a sFU to the interference power received from a cFCBS closest to that sFU, i.e., a cFCBS at the minimum distance. The minimum distance of a cFCBS from any sFUs is $d_{\min}$ =5 m in intra-floor level, whereas the minimum vertical distance of a cFCBS is $d_{\text{ver,min}}$ = 3 m in inter-floor level as shown in Fig. 3. The interference power from each cFCBS is normalized such that $\forall \psi\ \alpha_{\psi} \in [0,1]: \alpha_1 = \alpha_2 =,\ldots,= \alpha_{\psi_{\text{m}}} = \alpha_{\text{tra}}$ for intra-floor interference power and $\forall \psi\ \alpha_{\psi} \in [0,1]: \alpha_1 = \alpha_2 =,\ldots,= \alpha_{\psi_{\text{m}}} = \alpha_{\text{ter}}$ for inter-floor interference power received from any cFCBSs ψ of any tiers where ψ_{m} denotes the maximum number of cFCBSs per tier. Hence, the normalized aggregate intra-floor interference power at a sFU can be expressed as

$$\alpha_{\text{agg,tra}} = \sum_{\psi=1}^{\psi_{\text{m}}} 1_{r_{\psi}} \left(\alpha_{\psi}\right) \times \alpha_{\psi}$$

where $r_{\psi} \in \left\{\alpha_1, \alpha_2, \alpha_3, ..., \alpha_{\psi_{\text{m}}}\right\}$. 1(.) defines that 1(.) = 1 if α_{ψ} exists in the set r_{ψ} for any ψ, otherwise 1(.) = 0.

Using the 3GPP indoor path loss model of FCBSs [27, 29] and considering the interference effect of cFCBSs of the first-tier and the maximum transmit power of 20 dBm of any FCBSs, the normalized value of intra-floor interference power at an arbitrary distance d_{tra} from a cFCBS at a sFU is given by [26],

$$\alpha_{\text{tra}}\left(d_{\text{tra}}\right) = \left(d_{\min}/d_{\text{tra}}\right)^3 \tag{1}$$

where $d_{\min}$ is the minimum (or reference) distance between any cFCBSs and a sFU.

The proof of Eq. (1) is given in the following in Proof 1 [26].

Proof 1: The CCI power (dBm) at a sFU from a cFCBS at d_{tra} is given by,

$$\alpha_{\text{c,tra}}\left(d_{\text{tra}}\right) = P_t - PL\left(d_{\text{tra}}\right) = 20 - \left(127 + 30\log_{10}\left(d_{\text{tra}}/1000\right)\right)$$

where, in general, P_t and $PL\left(d_{\text{tra}}\right)$ respectively denote the transmit power of any FCBSs and the distant-dependent path loss between any FCBSs and any sFUs at d_{tra} from the FCBS.

Solving for $\alpha_{\text{c,tra}}\left(d_{\text{tra}}\right)$ yields the following.

$$\alpha_{\text{c,tra}}\left(d_{\text{tra}}\right) = 10^{-\left(10.7+3\log_{10}\left(d_{\text{tra}}/1000\right)\right)}$$

As aforementioned, considering only the first tier of cFCBSs around a sFCBS, the maximum value of CCI from a cFCBS is given by,

$$\alpha_{\text{max,tra}}\left(d_{\min}\right) = 10^{-\left(10.7+3\log_{10}\left(d_{\min}/1000\right)\right)}$$

Hence, the normalized value of intra-floor interference from a cFCBS at a sFU is given by,

$$\alpha_{\text{tra}}\left(d_{\text{tra}}\right) = \alpha_{\text{c,tra}}\left(d_{\text{tra}}\right)/\alpha_{\text{max,tra}}\left(d_{\text{tra}}\right)$$

Solving for $\alpha_{\text{tra}}\left(d_{\text{tra}}\right)$ yields the following.

$$\alpha_{\text{tra}}\left(d_{\text{tra}}\right)=\left(d_{\min}/d_{\text{tra}}\right)^{3} \quad \blacksquare$$

Using the same conditions as in intra-floor interference modeling and a floor attenuation factor $\alpha_{\text{f}}(d_{\text{ter}})$, the normalized value of inter-floor interference power for an arbitrary inter-floor distance d_{ter} at a sFU from a cFCBS located on a floor other than that of the sFCBS is given by [26],

$$\alpha_{\text{ter}}\left(d_{\text{ter}}\right)=10^{-(0.1\alpha_{\text{f}}(d_{\text{ter}}))}\left(d_{\min}/d_{\text{ter}}\right)^{3} \tag{2}$$

where the variation in $\alpha_{\text{f}}(d_{\text{ter}})$ is modeled such that the measured signal decreases by about 12 dB per floor for the first 6 floors of separation and an average of 1.35 dB per floor from floors 7 to 12. For any floors 13 and beyond, a random value [0, 1] in dB is considered. Also, d_{ter} of a cFCBS from a sFU can be expressed as $d_{\text{ter}}=\sqrt{{d_{\min}}^{2}+{d_{\text{ver}}}^{2}}$ where d_{ver} is the vertical distance between a sFCBS and any cFCBSs on a floor other than that of the sFCBS. The proof of Eq. (2) is given in the following in Proof 2 [26].

Proof 2: Following $\alpha_{\text{c,tra}}\left(d_{\text{tra}}\right)$, the CCI power (dBm) at a sFU from a cFCBS at d_{ter} in inter-floor level, $\alpha_{\text{c,ter}}\left(d_{\text{ter}}\right)$ can be expressed as follows:

$$\alpha_{\text{c,ter}}\left(d_{\text{ter}}\right)=10^{-\left(10.7+3\log_{10}\left(d_{\text{ter}}/1000\right)+\alpha_{\text{f}}\left(d_{\text{ter}}\right)/10\right)}$$

Also, the normalized received power at a sFU in inter-floor level is given by,

$$P_{\text{r,ter}}\left(d_{\text{ter}}=d_{\min}\right)=10^{-\left(10.7+3\log_{10}\left(d_{\min}/1000\right)\right)}$$

Hence, the normalized CCI power $\alpha_{\text{ter}}\left(d_{\text{ter}}\right)$ from any cFCBSs on any floors other than the floor of the sFU is given by,

$$\alpha_{\text{ter}}\left(d_{\text{ter}}\right)=\alpha_{\text{c,ter}}\left(d_{\text{ter}}\right)/P_{\text{r,ter}}\left(d_{\text{ter}}\right)$$

Solving for $\alpha_{\text{ter}}\left(d_{\text{ter}}\right)$ yields the following.

$$\alpha_{\text{ter}}\left(d_{\text{ter}}\right)=10^{-(0.1\alpha_{\text{f}}(d_{\text{ter}}))}\left(d_{\min}/d_{\text{ter}}\right)^{3} \quad \blacksquare$$

In a 3D multi-floor building, since cFCBSs are present in both intra-floor and inter-floor levels, the total aggregate interference power at a sFU is given as follows such that $\alpha_{\text{agg,ter}}+\alpha_{\text{agg,tra}}\le\alpha_{\text{thr,ter}}+\alpha_{\text{thr,tra}}$.

$$\begin{aligned}\alpha_{\text{agg,tot}}&=\alpha_{\text{agg,ter}}+\alpha_{\text{agg,tra}}\\ \alpha_{\text{agg,tot}}&=10^{-(\alpha_{\text{f}}(d_{\text{ter}})/10)}\,y_{\max,\text{ter}}\left(d_{\min}/d_{\text{ter}}\right)^{3}+y_{\max,\text{tra}}\left(d_{\min}/d_{\text{tra}}\right)^{3}\end{aligned}$$

where $\alpha_{\text{agg,tra}}$ and $\alpha_{\text{agg,ter}}$ denote respectively an aggregate interference power received at a sFU from intra-floor and inter-floor cFCBSs.

3.2.2. RoE modeling

The RoE of cFCBSs depends mainly on the following factors.

1. Optimization constraints to enforce a RoE, e.g. link spectral efficiency constraints, such that $\sigma_{\text{tra,se}} \geq \sigma_{\text{thr,se}}$ in intra-floor level and $\sigma_{\text{ter,se}} \geq \sigma_{\text{thr,se}}$ in inter-floor level. $\sigma_{\text{thr,se}}$ denotes the spectral efficiency constraint, the value of which is upper limited by 4.4 bps/Hz for a link signal-to-interference-plus-noise-ratio $\rho_{\text{tra}} \geq 22\,\text{dB}$ such that the value of $\sigma_{\text{thr,se}}$ can be varied from 0 bps/Hz to 4.4 bps/Hz.
2. Transmit power per FCBS $P_{\text{T}} \leq P_{\text{T,max}}$ where $P_{\text{T,max}}$ is the maximum transmit power of a FCBS.
3. Operating frequency of each FCBS, either a single band $\{f_{\text{fcbs}} : f_{\text{fcbs}} \in f_1 \vee f_2\}$ or multi-band $\{f_{\text{fcbs}} : f_{\text{fcbs}} \in f_1 \wedge f_2\}$ such that $\{f_{\text{fcbs}} : f_{\text{fcbs}} \in f_1 \vee f_2 \vee \{f_1 \wedge f_2\}\}$. Note that f_1 and f_2 denote operating frequencies of a FCBS at different bands.
4. Operating frequencies of the MCBS and FCBSs, either at the same co-channel low frequency, i.e. $f_{\text{fcbs}} = f_{\text{mcbs}}$, or a different high frequency, i.e. $f_{\text{fcbs}} > f_{\text{mcbs}}$, such that $\{f_{\text{fcbs}} : f_{\text{fcbs}} \geq f_{\text{mcbs}}\}$. f_{mcbs} denotes the operating frequency of the MCBS.
5. C-/U-plane architectures of FCBSs $\{a_{\text{arch}} : a_{\text{arch}} \in a_{\text{cuca}} \vee a_{\text{cusa}}\}$ where a_{cuca} and a_{cusa} denote CUCA and CUSA respectively.

Hence, mathematically an optimal RoE can be found by solving the following optimization problem for the given factors 3, 4, and 5.

$$\begin{aligned} &\text{minimize} && \Theta_{\text{RoE}} \\ &\text{such that} && \sigma_{\text{tra,se}} \geq \sigma_{\text{thr,se}} \\ & && \sigma_{\text{ter,se}} \geq \sigma_{\text{thr,se}} \\ & && P_{\text{T}} \leq P_{\text{T,max}} \end{aligned}$$

where Θ_{RoE} denotes the number of FCBSs per RoE in a building. Note that the minimization is considered because the smaller the RoE, the more the resource reuse times for the same set of FCBSs per building.

Since Θ_{RoE} in a 3D multi-floor building can be defined by an optimal minimum distance d_{tra}^* for intra-floor level as well d_{ter}^* for inter-floor level to reuse resources in both intra-and inter-floor cFCBSs, the above optimization problem for Θ_{RoE} can be solved in terms of d_{tra} and d_{ter} by separating the problem into two sub-problems where sub-problem 1 is for finding a solution of d_{tra}, and sub-problem 2 is for finding a solution of d_{ter} as follows.

Sub-problem 1:

$$\begin{aligned} &\text{minimize} && d_{\text{tra}} \\ &\text{such that} && \sigma_{\text{tra,se}} \geq \sigma_{\text{thr,se}} \\ & && P_{\text{T}} \leq P_{\text{T,max}} \end{aligned}$$

Sub-problem 2:

$$\begin{aligned} &\text{minimize} && d_{\text{ter}} \\ &\text{such that} && \sigma_{\text{ter,se}} \geq \sigma_{\text{thr,se}} \\ & && P_{\text{T}} \leq P_{\text{T,max}} \end{aligned}$$

For the maximum transmit power of a FCBS, the solutions of d_{tra}^* and d_{ter}^* for $\alpha_{\text{agg,tra}} >> N^{\text{s}}$ and $\alpha_{\text{agg,ter}} >> N^{\text{s}}$ are given by [26],

$$d_{\text{tra}}^* \geq d_{\min}\left(y_{\text{max,tra}}\left(2^{\sigma_{\text{thr,se}}} - 1\right)\right)^{1/3} \tag{3}$$

$$d_{\text{ter}}^* \geq d_{\min}\left(10^{-\left(0.1\alpha_{\text{f}}\left(d_{\text{ter}}^*\right)\right)} y_{\text{max,ter}}\left(2^{\sigma_{\text{thr,se}}} - 1\right)\right)^{1/3} \tag{4}$$

where $N^{s} \in [0,1]$ denotes the normalized noise power. The maximum number of cFCBSs $y_{\max,\text{tra}} = 8$ for intra-floor interference, whereas the maximum number of cFCBSs $y_{\max,\text{ter}} = 1$ for single-sided cFCBSs, and $y_{\max,\text{ter}} = 2$ for double-sided cFCBSs for inter-floor interference. The proofs of Eq. (3) and Eq. (4) are given in the following in Proof 3 and Proof 4 respectively [26].

Proof 3: An intra-floor link capacity in bps/Hz for the link capacity σ_{tra} in bps and an arbitrary bandwidth Ξ_{tra} can be expressed as

$$\sigma_{\text{tra,se}} = \sigma_{\text{tra}} / \Xi_{\text{tra}} = \log_2\left(1 + 1/\left(\alpha_{\text{agg,tra}} + N^{s}\right)\right)$$

However, $\sigma_{\text{tra,se}} \geq \sigma_{\text{thr,se}}$ is satisfied when $d_{\text{tra}} \geq d^{*}_{\text{tra}}$, such that the above expression can be written as

$$\log_2\left(1 + 1/\left(y_{\max,\text{tra}}\left(d_{\min}/d^{*}_{\text{tra}}\right)^{3} + N^{s}\right)\right) \geq \sigma_{\text{thr,se}}$$

Solving for d^{*}_{tra} for $\alpha_{\text{agg,tra}} >> N^{s}$ yields the following.

$$d^{*}_{\text{tra}} \geq d_{\min}\left(y_{\max,\text{tra}}\left(2^{\sigma_{\text{thr,se}}} - 1\right)\right)^{1/3}$$

Similarly, an inter-floor link capacity in bps/Hz for the link capacity σ_{ter} in bps and an arbitrary bandwidth Ξ_{ter} can be expressed as

$$\sigma_{\text{ter,se}} = \sigma_{\text{ter}} / \Xi_{\text{ter}} = \log_2\left(1 + 1/\left(\alpha_{\text{agg,ter}} + N^{s}\right)\right)$$

But, $\sigma_{\text{ter,se}} \geq \sigma_{\text{thr,se}}$ is satisfied when $d_{\text{ter}} \geq d^{*}_{\text{ter}}$, such that the above expression can be written as

$$\log_2\left(1 + 1/\left(10^{-(0.1\alpha_{\text{f}}(d_{\text{ter}}))}\, y_{\max,\text{ter}}\left(d_{\min}/d^{*}_{\text{ter}}\right)^{3} + N^{s}\right)\right) \geq \sigma_{\text{thr,se}}$$

Solving for d^{*}_{ter} for $\alpha_{\text{agg,ter}} >> N^{s}$ yields the following.

$$d^{*}_{\text{ter}} \geq d_{\min}\left(10^{-\left(0.1\alpha_{\text{f}}\left(d^{*}_{\text{ter}}\right)\right)}\, y_{\max,\text{ter}}\left(2^{\sigma_{\text{thr,se}}} - 1\right)\right)^{1/3}$$ ■

Since d^{*}_{tra} and d^{*}_{ter} are independent of the number of reused RBs in a cFCBS, any numbers of RB can be reused in cFCBSs that are located from one another at distances at least $d_{\text{tra}} \geq d^{*}_{\text{tra}}$ for intra-floor level and $d_{\text{ter}} \geq d^{*}_{\text{ter}}$ for inter-floor level. Note that since we adopt the solutions from [26], each proof of the solutions given by Eq. (1)-Eq. (4) is provided in brief above, and a detailed derivation of each proof can be found in [26]. In addition, a more detail explanation on intra-and inter-floor interference modeling can be found in [26]. Hence, a 3D RoE $\Theta_{\text{RoE,3D}}$ of any cFCBSs then can be formed using d^{*}_{tra} and d^{*}_{ter} as follows.

Let $\kappa_{\max,\text{tra}}$ denote the maximum number of tiers of FCBSs with orthogonal frequencies within the RoE of any cFCBSs in intra-floor level, which can be given by,

$$\kappa_{\max,\text{tra}} = \text{ceil}\left(d^{*}_{\text{tra}} + \left(a/2\right)/a\right)$$

where a =10 m is the length of an edge of any square apartments.

Hence, the RoE around any cFCBSs in intra-floor level in terms of the number of FCBSs can be found as follows.

$$\Theta_{\mathrm{RoE,tra}} = \sum_{\kappa=1}^{\kappa_{\mathrm{max,tra}}} 8\times\kappa$$

Similarly for the inter-floor level, the maximum number of tiers of FCBSs with orthogonal frequencies within the RoE of any cFCBSs is given by,

$$\kappa_{\mathrm{max,ter}} = \mathrm{ceil}\left(d_{\mathrm{ter}}^{*}/d_{\mathrm{ver}}\right)$$

Hence, a 3D RoE of any cFCBSs can be found as follows.

$$\Theta_{\mathrm{RoE,3D}} = \left(y_{\mathrm{max,ter}}\times\kappa_{\mathrm{max,ter}}\right)\times\Theta_{\mathrm{RoE,tra}}$$

where $y_{\mathrm{max,ter}} = 1$ for single-sided cFCBSs and $y_{\mathrm{max,ter}} = 2$ for double-sided cFCBSs in inter-floor level. In Fig. 3, $\Theta_{\mathrm{RoE,tra}} = 8\times1 = 8$, $\kappa_{\mathrm{max,ter}} = \mathrm{ceil}(6/3) = 2$ such that for $y_{\mathrm{max,ter}} = 1$, $\Theta_{\mathrm{RoE,3D}} = (1\times2)\times8 = 16$. Since $\kappa_{\mathrm{max,ter}} = 2$, frequency resources can be reused in every alternate floor of the building as shown in Fig. 3.

4. In-Building FCBS Clustering and Resource Reuse Approach

4.1. FCBS Clustering Approach

A cluster of FCBSs can be formed based on the RoE as modeled in the previous section constrained by the link spectral efficiency in both intra-and inter-floor levels as follows. The cluster size of a cFCBS in intra-floor level can be expressed as follows.

$$\Theta_{\mathrm{cl,tra}} = \sum_{\kappa=()}^{\kappa_{\mathrm{max,tra}}} (1+2\kappa)$$

Hence, the 3D cluster size of any cFCBSs in a multi-storage building can be found as follows.

$$\Theta_{\mathrm{cl,3D}} = \left(y_{\mathrm{max,ter}}\times\kappa_{\mathrm{max,ter}}\right)\times\Theta_{\mathrm{cl,tra}}$$

Figure 4 shows an illustrative formation of a 3D cluster of FCBSs in a multi-floor building using the link spectral efficiency constraint based resource reuse graph with respect to the floor *fl*+1. Each node represents a cFCBS, and each edge represents the constraint that is to be satisfied to reuse resources in cFCBSs. Note that clusters of FCBSs in both intra-and inter-floor levels are shown in red color lines; edges in blue color represent that the constraint is satisfied to reuse the same frequency resources; ash color circles represent cFCBSs. Hence, frequency resources can be reused in every 3 FCBSs in intra-floor level and every alternate floors in inter-floor level in Fig. 4. Note that with a change in the constraint value, the size of a cluster varies. Since we consider the same value of spectral efficiency constraint for all clusters in both intra-and inter-floor levels, all 3D clusters within a building comprise of the same number of FCBSs for a given constraint. However, the size of each cluster in different buildings may vary with different values of the constraint.

DOI:10.4186/ej.2017.21.3.309

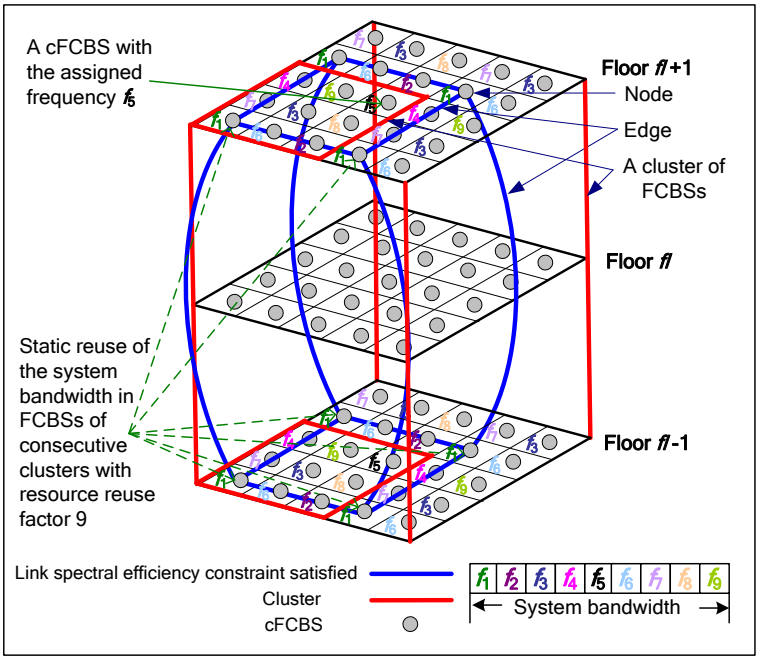

Fig. 4. FCBS clustering with a static allocation and reuse of the available frequency in FCBSs deployed in a building.

4.2. FCBS Resource Reuse Approach

We consider reusing the available frequency of each FCBS architecture in each cluster (Fig. 4) following a static frequency allocation scheme to avoid CCI such that all FCBSs within a cluster are cFCBSs with respect to all neighbouring clusters. Each FCBS within a cluster is allocated to the same amount of frequency. Hence, the frequency allocation to each FCBS within a cluster is static, i.e. the frequency allocated to any FCBS r of any cluster cl, $S_{r,cl}$, can only be allocated to the FCBS r of the neighbouring cluster $(cl+n)$, $S_{r,cl+n}$, such that $S_{r,cl}=S_{r,cl+n}$ where n=1, 2, 3,…, $cl_{\max}$, and $cl_{\max}$ denotes the maximum number of clusters that can be formed within a 3D building. Hence, because of reusing the same frequency in contiguous clusters, frequency resources of any FCBS r of cluster cl, $S_{r,cl}$, cannot be allocated to other FCBSs than r of any neighbouring cluster $(cl+n)$ even though there is less or no traffic demand from the FCBS r of cluster $(cl+n)$ in any TTIs.

Though the reuse of RBs becomes dependent on the deployment of FCBSs within any clusters because of static and regular pattern of RB allocations in FCBSs per cluster, the whole available frequency can be reused in FCBSs within each cluster, and hence the capacity and spectral efficiency increase with a decrease in cluster size for a given frequency resource. Further, since all FCBSs in all clusters gain advantages from the link spectral efficiency constraint enforced by an optimizer, the overall capacity gain from such static resource reuse approach is expected to be higher than that achieved with techniques where resources of one cluster is reused opportunistically to another, and clusters are relatively far apart from one another to avoid CCI. Furthermore, because of an equal number of RBs allocated to each FCBS within a cluster, like Round Robin scheduler, the maximum fairness factor of unity can be achieved.

In the following, we propose an algorithm for a non-adjacent static RB allocation in FCBSs with CUCA per cluster to avoid adjacent channel interference (ACI). The extension for CUSA is straightforward based on the number of transceivers and frequency bands per FCBS as described above. Since the enforced constraints in both intra-and inter-floor levels must be satisfied, the total available bandwidth must first be divided by the number of floors fl_{3DR} within a cluster for inter-floor level constraint. A set of an equal number of RBs in the bandwidth is then allocated to each FCBS within each cluster spanning across fl_{3DR} floors. The algorithm is described in a number of steps as follows in Algorithm 1.

Algorithm 1. Proposed ACI avoided static RB resource reuse and allocation to FCBSs with CUCA in a 3D building.

Step 1: Divide the total number of RBs M_T of the system bandwidth into fl_{3DR} sets of consecutive RBs such that $M = M_T / fl_{3DR}$ consecutive RBs are allocated and reused in FCBSs of each 3D cluster spanning across fl_{3DR} floors to satisfy the inter-floor spectral efficiency constraint (Fig. 5(a)).

Step 2: Now divide M for any floors within a cluster into two sets of consecutive RBs denoted as {i} and {j} such that $m_d = \{\{i\},\{j\}\}$ and $|m_d| = M$. Let $m_d = \{1,2,\cdots,M\}$ denote a set of RB indices such that the following holds (Fig. 5(a)):

$$\begin{aligned} |i| &= |j| + 1, \quad \text{if } M/2 \text{ is a non} - \text{integer} \\ |i| &= |j|, \quad\quad \text{if } M/2 \text{ is an integer} \end{aligned}$$

So that $i = \{1,2,\cdots,(M/2) + x_v\}$

$j = \{(M/2)+1,(M/2)+2,\cdots,M\}$

where $x_v = 1$ for $|i| > |j|$, and $x_v = 0$ for $|i| = |j|$.

Step 3: Find the value of the number of FCBSs n_{diag} along the diagonal of the set of square grid apartments on the 2D space of any floors within the cluster.

Step 4: Estimate the total number of FCBSs per floor in a 3D cluster, given by the following expression.

$$n_{cl} = n_{diag} + 2\sum_{y=1}^{y=(n_{diag}-1)} (n_{diag} - y)$$

Step 5: Estimate the total number of orthogonal sets of RBs in m_d, which can be found by the following expression.

$$m_{orth} = n_{diag} + (n_{diag} - 1) = 2n_{diag} - 1$$

Step 6: Form the orthogonal sets of RBs m_{orth} such that the sets {i} and {j} include subsets of consecutive RB indices of the sizes as follows (Fig. 5(b)).

$$i = \{1,3,5,\cdots,n_{diag}-1,n_{diag}-3,n_{diag}-5,\cdots,5,3,1\}$$

$$j = \{2,4,6,\cdots,n_{diag},n_{diag}-2,n_{diag}-4,\cdots,6,4,2\}$$

where each entry in {i} and {j} represents the number of consecutive RB indices, i.e. the size of the corresponding subset of RB indices.

Step 7: Now allocate consecutive subsets of RB indices to FCBSs alternatively starting from set {i} to {j}, then back to{i} to {j} again, and so on until the last subset of either {i} or {j} reaches (Fig. 5(c)). RB indices are allocated to FCBSs starting from the lower triangle heading towards the diagonal and then to the upper triangle of the square cluster so that adjacent RB indices are not allocated to contiguous FCBSs to avoid ACI. All these steps are explained with an example in the following in Example 1. Note that all FCBSs in all clusters in a multi-floor building are allocated by RBs following the same and fixed pattern using the aforementioned Steps 1 through 7.

Step 8: Since the total number of RBs in the system bandwidth M_T is reused in all floors per cluster with M RBs per floor, and each floor has the same number of FCBSs, the total number of times M_T can be reused per building can be found by dividing the total number of floors in a building fl_T by the number of floors per 3D cluster fl_{3DR}. Note that with 3D cluster, we define a cluster that satisfies spectral efficiency constraints in both intra-floor and inter-floor levels. Let cl_{intra} denote the number of FCBSs per

floor in a 3D cluster, and S_F denote the total number of FCBS per building. The resource reuse factor (i.e., the number of FCBSs per 3D cluster) is then given by,

$$\xi_f = fl_{3DR} \times cl_{intra}$$

Also, the resource reuse times can be given by,

$$\xi_t = S_F / \xi_f .$$

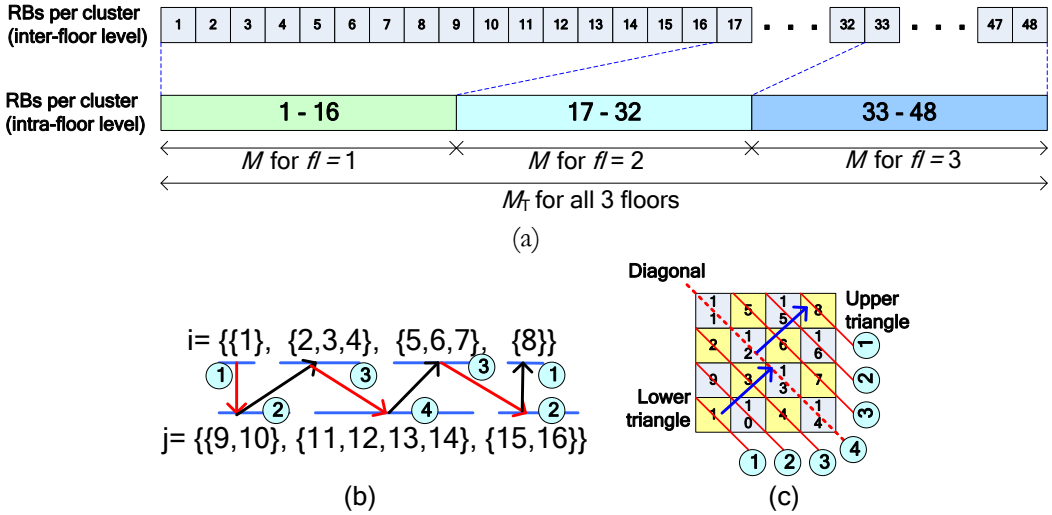

Fig. 5. Static RB resource allocation to FCBSs with ACI avoidance: (a) M_T = 48 for inter-floor level; (b)-(c) M=16 for intra-floor level.

Example 1: Let M_T =48, fl_{3DR}=3, cl_{intra}=4, and fl_T=15.

Step 1: $M = 48/3 = 16$, i.e. each inter-floor level cluster has 16 FCBSs.

Step 2: $m_d = \{1,2,\cdots,16\}$, and $M/2 = 16/2 = 8$ is an integer. Hence,

$$i = \{1,2,3,4,5,6,7,8\}$$
$$j = \{9,10,11,12,13,14,15,16\}$$

Step 3: for M=16, $n_{diag} = 4$.

Step 4: $n_{cl} = 4 + 2\sum_{y=1}^{y=3}(4-y) = 4 + 2\cdot(3+2+1) = 16$.

Step 5: the total number of orthogonal sets of RBs, $m_{orth} = (2\times 4) - 1 = 7$

Step 6: for m_{orth} orthogonal sets of RBs, the sets {i} and {j} include subsets of consecutive RB indices of the sizes:

$$i = \{1,3,3,1\}$$
$$j = \{2,4,2\}$$

such that RB indices in subsets are as follows.

$$i = \{\{1\},\{2,3,4\},\{5,6,7\},\{8\}\}$$
$$j = \{\{9,10\},\{11,12,13,14\},\{15,16\}\}$$

Step 7: allocate consecutive subsets of RB indices to FCBSs alternatively starting from set {i} to {j} to avoid adjacent RB interference.

Step 8: the resource reuse factor $\xi_f = fl_{3DR} \times cl_{intra} = 3\times 4 = 12$, and resource reuse times $\xi_t = S_F/\xi_f = 250/12 = 20.83$. Hence, the spectral efficiency can be improved by 20.83 times because of reusing resources in FCBSs.

Note that in intra-floor level (Fig. 5(c)), there is no contiguous RB indices allocated to FCBSs next to one another except those FCBSs at the edge point along the diagonal of each apartment. However, such effect is negligible as compared to the non-adjacent RB allocations around each side of each square apartment. For inter-floor level, orthogonal set of RBs are allocated to each floor within the cluster.

5. Multi-Tier System Architecture and Interference Management

5.1. Multi-Tier System Architecture

5.1.1. Base station and user distribution

We consider a multi-tier network for both CUCA and CUSA as illustrated in Fig. 6, which consists of a single MCBS of a corner excited 3-sectored MC site and a number outdoor PCs and indoor FCs deployed in a number of multi-storage buildings in an urban environment. A certain percentage of MUs are considered within buildings, and a few outdoor MUs are offloaded to nearby PCBSs. All MUs are partitioned randomly into three disjoint subsets of indoor, outdoor, and offloaded MUs. Each FC serves one FU, and an offloaded MU to any PCBSs is equally likely in a realization. PCs and multi-storage buildings of FCs are located randomly and uniformly within the coverage of the MC. Outdoor MUs, offloaded MUs, and FUs are distributed randomly and uniformly within their respective BSs' coverages. However, to define a RoE, a FU is considered to locate at the farthest radial distance from its sFCBS for the worst-case analysis.

5.1.2. Backhaul

In Fig. 6, backhauls in green color carry both C-/U-plane traffic, and backhauls in red color carry only C-plane traffic. Unlike CUCA, separate backhauls for C-/U-plane traffic are needed for CUSA. Hence, backhauls in green color in Fig. 6 for the MCBS and PCBSs need to be split into two, one for C-plane and the other for U-plane traffic. However, FCBSs carry only the U-plane traffic when operating at a single band. For multiple bands enabled FCBSs, separate C-/U-plane backhauls are needed. The MCBS and each cluster of FCBSs in a building are connected to each other via an X2 backhaul through a FCBS gateway to coordinate resource allocation for interference management and UE association.

5.2. Multi-Tier Interference Management

Assume that the path loss because of the distance between buildings and the external wall penetration loss of a building are significant enough such that the CCI effect from reusing the same frequency in FCBSs of different buildings is negligible. Hence, the whole system bandwidth can be reused in FCBSs of each building for a co-channel operated FCBS. All UEs are allocated orthogonally to RBs in their respective tier. Offloaded and outdoor MUs can transmit in all TTIs. A MU can be detected whether or not within any buildings using techniques such as measuring its downlink path loss such that a sudden fall in the received signal strength at the MU can be observed when moving into a building because of a high external wall penetration loss of the building. To avoid the cross-tier CCI, an orthogonal allocation of RBs in time-domain is considered between indoor MUs and FUs, i.e. indoor MUs can be served only during ABSs, while FCBSs can transmit only during non-ABSs of the ABS based eICIC. For a different frequency operated FCBS, we consider 60-GHz mmWave band, and there is no need for the cross-tier interference management between any indoor MUs and FUs because of operating the MCBS and FCBSs at different frequencies.

DOI:10.4186/ej.2017.21.3.309

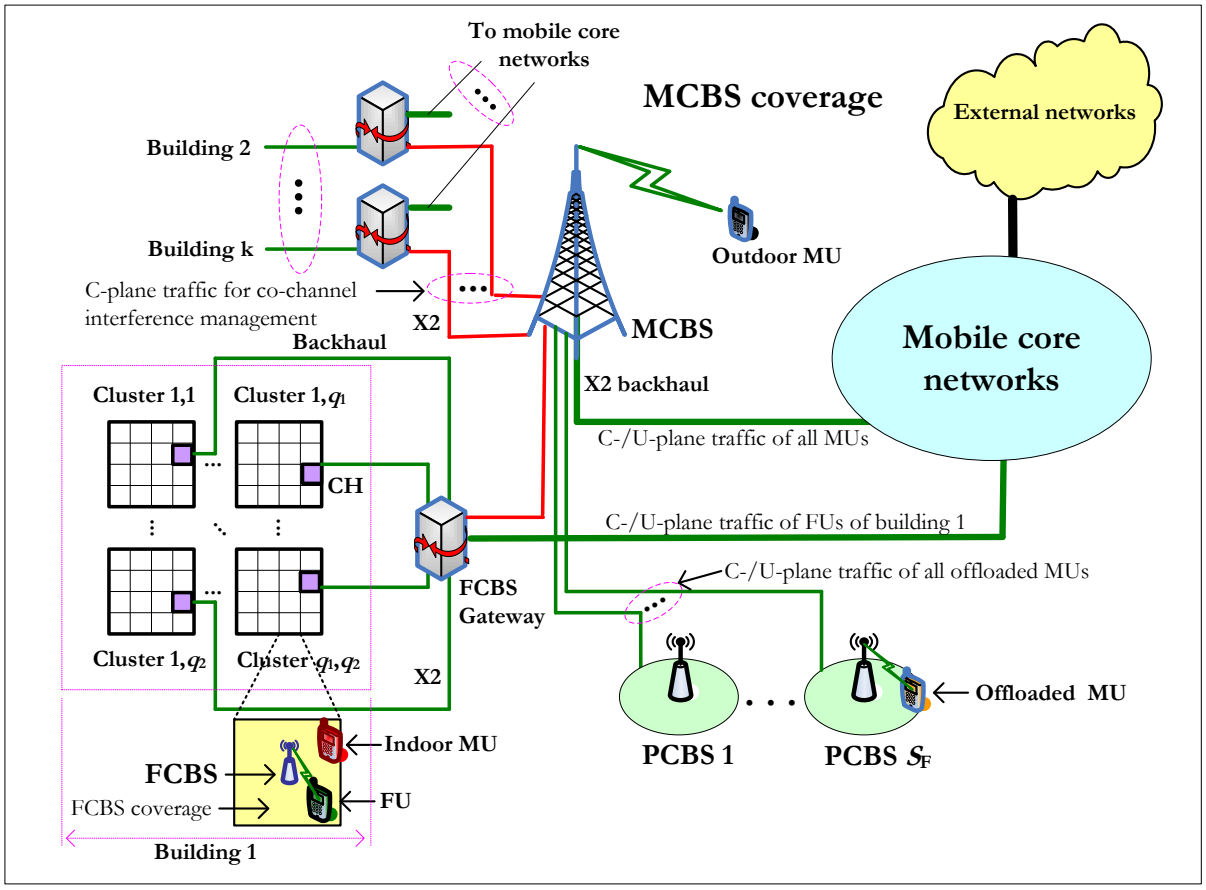

Fig. 6. System architecture of a multi-tier network.

6. Problem Formulation

6.1. Multi-Tier Network Model

Consider that there are N MUs in the system. Let S_P denote the number of PCs in the MC coverage. Consider that the number of offloaded MUs is uniformly distributed in the interval [1, U_{OFL}]. If all PCs have an equal number of offloaded MUs U_P, i.e. $\forall q U_P^q = U_P$, then the total number of offloaded MUs, $U_{OFL}=S_P \times U_P$. However, in general, U_P^q is a random variable, which varies from one PC to another, and the realization of U_P^q for a PC is mutually independent from the others. If μ_{MI} denotes the ratio of the number of indoor MUs, then the total number of indoor MUs is $U_{MI}=\mu_{MI} \times N$, outdoor MUs served by the MC is $U_{MO}= N-U_{OFL}-U_{MI}$, total outdoor MUs served by the MC and PCs is $U_{MP}= U_{MO}+U_{OFL}$, and total MUs served by the MC is $U_M=U_{MO}+U_{MI}$.

Let $\boldsymbol{N}_M$ denote the set of indices of all MUs such that $\boldsymbol{N}_M=\{1, 2, 3, \ldots, N\}$. Denote $\boldsymbol{N}_{MO}$, $\boldsymbol{N}_P$, and $\boldsymbol{N}_{MI}$ respectively the set of indices of all outdoor MUs, offloaded MUs, and indoor MUs. Note that $\boldsymbol{N}_M$ is partitioned randomly into three disjoint subsets $\boldsymbol{N}_{MO}$, $\boldsymbol{N}_P$, and $\boldsymbol{N}_{MI}$. Let L denote the maximum number of buildings in a MC coverage, and S_F denote the number of active FCs in each building. Assuming that S_F is the same for all buildings, the total number of active FCs in the system is $S_{FS}=L \times S_F$. Consider that the number of FUs in buildings are independent and uniformly distributed in the interval [1, U_F]. In general, U_F is a random variable that varies from one building to another, and the realization of U_F for a building is mutually independent from the others where a realization is defined as a simulation run time.

Let U_F^w denote the number of FUs served by a FC S_F^w in a building such that $\forall w U_F^w \in \left[0,\ U_{F,max}^w\right]$. If all FCs have an equal number of FUs U_{FU}, i.e. $\forall w U_F^w = U_{FU}$, then the total number of FUs in any buildings, $U_F=S_F \times U_{FU}$. However, in general, U_F^w is a random variable that varies from one FCBS to another, and the realization of U_F^w for a FCBS is mutually independent from the others. If each FC in a building serves one

UE, i.e. $U_{FU}=1$, the total number of FUs in a building is $U_F=S_F$, and in the system is $U_{FS}=L\times U_F$. Let $\boldsymbol{N_F}$ denote the set of all FU indices in a building such that $\boldsymbol{N_F}=\{1, 2, 3,\ldots, U_F\}$. The realization of MUs served by the MC and PCs are not mutually independent since MUs served by PCs are MUs offloaded from the MCBS, and the schedulers have a complete knowledge when a MU is offloaded. The indoor MUs are distributed randomly and non-uniformly within buildings.

Let $\boldsymbol{T}$ denote simulation run time with the maximum time of Q (in time step each lasting 1 ms) such that $\boldsymbol{T}=\{1, 2, 3,\ldots,Q\}$. Let $\boldsymbol{T_{ABS}}$ denote the number of ABSs in every ABS pattern period (APP) of 8 subframes such that $\boldsymbol{T_{ABS}}\subseteq\boldsymbol{T}$ and $\boldsymbol{T_{ABS}}=\{t: t=8v+z; v=0, 1, 2,\ldots,Q/8; z=1,\ldots,T_{ABS}\}$ where $T_{ABS}=1, 2,\ldots,8$ corresponds to ABS patterns $\phi=1/8, 2/8,\ldots, 8/8$ respectively. Let t_{ABS} and $t_{non-ABS}$ denote respectively an ABS and a non-ABS such that $t_{ABS}\in\boldsymbol{T_{ABS}}$ and $t_{non-ABS}\in\boldsymbol{T}\setminus\boldsymbol{T_{ABS}}$.

6.2. Capacity Formulation

Let d_{MU}, d_{PC}, and d_{FCL} denote respectively the distances of any MUs, PCs, and buildings from the MCBS, and d_{FC} denote the distance between a FCBS and a FU. The distances of all UEs of each category in a realization are generated following the respective distribution functions as mentioned earlier. The received signal-to-interference-plus-noise ratio for a UE at RB=i in TTI=t can be expressed as

$$\rho_{t,i}=\left(P_{t,i}/(N^s_{t,i}+I_{t,i})\right).H_{t,i} \tag{5}$$

where $P_{t,i}$ is the transmit power, $N^s_{t,i}$ is the noise power, $I_{t,i}$ is the total interference signal power, and $H_{t,i}$ is the link loss for a link between a UE and a BS at RB=i in TTI=t. $H_{t,i}$ can be expressed in dB as

$$H_{t,i}(\text{dB})=(G_t+G_r)-(L_F+PL_{t,i})+(LS_{t,i}+SS_{t,i}) \tag{6}$$

where (G_t+G_r) and L_F are respectively the total antenna gain and connector loss. $LS_{t,i}$, $SS_{t,i}$, and $PL_{t,i}$ respectively denote large scale shadowing effect, small scale Rayleigh or Rician fading, and distance dependent path loss between a BS and a UE at RB=i in TTI=t.

Using Shannon's capacity formula, a link throughput at RB=i in TTI=t in bps per Hz is given by [30-31],

$$\sigma_{t,i}(\rho_{t,i})=\begin{cases}0, & \rho_{t,i}<10\,\text{dB}\\ \beta\log_2\left(1+10^{(\rho_{t,i}(\text{dB})/10)}\right), & 10\,\text{dB}\le\rho_{t,i}\le 22\,\text{dB}\\ 4.4, & \rho_{t,i}>22\,\text{dB}\end{cases} \tag{7}$$

where β is considered as the implementation loss factor.

Let M_T and m_T denote respectively the number of RBs in microwave and mmWave bandwidths where an RB is equal to 180 kHz such that in the following expressions, an arbitrary number of RBs must be multiplied by 180 kHz (not shown explicitly) to estimate the capacity in bps. The aggregate capacity of all MUs for M_T RBs and Q TTIs can be expressed as

$$\sigma_{MC}=\sum_{t=1}^{Q}\sum_{i=1}^{M_T}\sigma_{t,i}(\rho_{t,i}) \tag{8}$$

where σ and ρ are responses over M_T RBs of only indoor MUs in $t\in\boldsymbol{T_{ABS}}$ and all outdoor and offloaded MUs in $t\in\boldsymbol{T}$.

Let U_{FC} denote the number of FCBSs per 3D cluster, and M_{FC} and m_{FC} denote an equal number of RBs per FCBS for microwave and mmWave bands respectively per 3D cluster such that the followings hold.

$$M_{\mathrm{T}} = U_{\mathrm{FC}} \times M_{\mathrm{FC}} \tag{9}$$

$$m_{\mathrm{T}} = U_{\mathrm{FC}} \times m_{\mathrm{FC}} \tag{10}$$

Let $\sigma_{\mathrm{thr,cc}}$ and $\sigma_{\mathrm{thr,df}}$ denote the required link spectral efficiencies between a sFU and its sFCBS within a cluster respectively for microwave and mmWave bands such that the required capacity constraints for each FCBS respectively for microwave and mmWave bands can be expressed as

$$\sigma_{\mathrm{thr,c,cc}} = M_{\mathrm{FC}} \times \sigma_{\mathrm{thr,cc}} \tag{11}$$

$$\sigma_{\mathrm{thr,c,df}} = m_{\mathrm{FC}} \times \sigma_{\mathrm{thr,df}} \tag{12}$$

Hence, the aggregate capacity from reusing M_{T} and m_{T} RBs in microwave and mmWave bands respectively per 3D cluster of U_{FC} FCBSs for Q TTIs can be given respectively by,

$$\begin{aligned} \sigma_{\mathrm{FC,cl,cc}} &= \sum_{t=1}^{Q} \sum_{i=1}^{M_{\mathrm{T}}} \sigma_{t,i}\left(\rho_{t,i}\right) \\ &= U_{\mathrm{FC}} \times \sigma_{\mathrm{thr,c,cc}} \times Q \\ &= U_{\mathrm{FC}} \times \left(M_{\mathrm{FC}} \times \sigma_{\mathrm{thr,cc}}\right) \times Q \end{aligned} \tag{13}$$

where σ and ρ are responses over M_{T} RBs of FUs per cluster in $t \in \boldsymbol{T} \setminus \boldsymbol{T}_{\mathbf{ABS}}$.

$$\begin{aligned} \sigma_{\mathrm{FC,cl,df}} &= \sum_{t=1}^{Q} \sum_{i=1}^{m_{\mathrm{T}}} \sigma_{t,i}\left(\rho_{t,i}\right) \\ &= U_{\mathrm{FC}} \times \sigma_{\mathrm{thr,c,df}} \times Q \\ &= U_{\mathrm{FC}} \times \left(m_{\mathrm{FC}} \times \sigma_{\mathrm{thr,df}}\right) \times Q \end{aligned} \tag{14}$$

where σ and ρ are responses over m_T RBs of FUs per cluster in $t \in \boldsymbol{T}$.

Hence, the aggregate capacity from reusing M_{T} and m_{T} RBs in microwave and mmWave bands per building for Q TTIs can be given respectively by,

$$\sigma_{\mathrm{FC,all,cc}} = \xi_{\mathrm{t,cc}} \times \left(U_{\mathrm{FC}} \times \left(M_{\mathrm{FC}} \times \sigma_{\mathrm{thr,cc}}\right) \times Q\right) \tag{15}$$

$$\sigma_{\mathrm{FC,all,df}} = \xi_{\mathrm{t,df}} \times \left(U_{\mathrm{FC}} \times \left(m_{\mathrm{FC}} \times \sigma_{\mathrm{thr,df}}\right) \times Q\right) \tag{16}$$

where $\xi_{\mathrm{t,cc}}$ and $\xi_{\mathrm{t,df}}$ denote resource reuse times respectively for microwave and mmWave bands per building.

6.2.1. FCBSs with CUSA

For a single transceiver based FCBSs with CUSA operating at the co-channel microwave, no FCBSs can transmit signals during an ABS. Hence, the aggregate capacity of all FUs per building for any ϕ and $\xi_{\mathrm{t,cc}}$ for Q TTIs is given by,

$$\begin{aligned} \sigma_{\mathrm{cusa,cc,s}} &= \left(1-\phi\right) \times \sigma_{\mathrm{FC,all,cc}} \\ &= \left(1-\phi\right) \times \xi_{\mathrm{t,cc}} \times \left(U_{\mathrm{FC}} \times \left(M_{\mathrm{FC}} \times \sigma_{\mathrm{thr,cc}}\right) \times Q\right) \end{aligned} \tag{17}$$

However, for a single transceiver based FCBSs operating at a different frequency mmWave, $\phi = 0$ such that the aggregate capacity of all FUs per building for $\xi_{\mathrm{t,df}}$ and Q TTIs is given by,

$$\begin{aligned}\sigma_{\text{cusa,df,s}} &= \sigma_{\text{FC,all,df}} \\ &= \xi_{\text{t,df}} \times \left(U_{\text{FC}} \times \left(m_{\text{FC}} \times \sigma_{\text{thr,df}}\right) \times Q\right)\end{aligned} \tag{18}$$

In a dual transceivers based FCBS with CUSA, since the mmWave serves U-plane traffic, the aggregate capacity of all FUs per building is the same as that of a single transceiver based different frequency mmWave enabled FCBS and is given by for Q TTIs,

$$\begin{aligned}\sigma_{\text{cusa,df,d}} &= \sigma_{\text{cusa,df,s}} \\ &= \xi_{\text{t,df}} \times \left(U_{\text{FC}} \times \left(m_{\text{FC}} \times \sigma_{\text{thr,df}}\right) \times Q\right)\end{aligned} \tag{19}$$

Note that the values of spectral efficiency constraint in microwave and mmWave bands are adjusted such that the cluster sizes at both bands are the same (i.e., $\xi_{\text{t,cc}} = \xi_{\text{t,df}}$) when FCBSs are enabled with dual transceivers.

6.2.2. FCBSs with CUCA

Let x_{cp} denote the percentage of C-plane traffic for FCBSs with CUCA in both microwave and mmWave bands. According to [32], the total control overhead includes 10% for S1 signaling, 4% for handover, and a certain percentages for management signaling. Hence, we assume x_{cp}=0.25 as an example. Since x_{cp} simply scales C-/U-plane traffic capacity, considering a different value will not change the trend of capacity responses. Hence, the aggregate capacity for a single transceiver based FCBSs with CUCA operating at the co-channel microwave and different frequency mmWave in a building can be given respectively for Q TTIs by,

$$\begin{aligned}\sigma_{\text{cuca,cc,s}} &= \left(1-x_{\text{cp}}\right) \times \left(1-\phi\right) \times \sigma_{\text{FC,all,cc}} \\ &= \left(1-x_{\text{cp}}\right) \times \left(1-\phi\right) \times \xi_{\text{t,cc}} \times \left(U_{\text{FC}} \times \left(M_{\text{FC}} \times \sigma_{\text{thr,cc}}\right) \times Q\right)\end{aligned} \tag{20}$$

and

$$\begin{aligned}\sigma_{\text{cuca,df,s}} &= \left(1-x_{\text{cp}}\right) \times \sigma_{\text{FC,all,df}} \\ &= \left(1-x_{\text{cp}}\right) \times \xi_{\text{t,df}} \times \left(U_{\text{FC}} \times \left(m_{\text{FC}} \times \sigma_{\text{thr,df}}\right) \times Q\right)\end{aligned} \tag{21}$$

6.2.3. Overall system capacity estimation

A) Single Band Different Frequency MmWave Enabled FCBSs

When FCBSs with CUCA operate at a single band different frequency mmWave, C-plane traffic of UEs is served by the respective BSs, i.e. MCBS for all MUs and FCBSs for FUs. However, for FCBSs with CUSA operating at a single band different frequency mmWave, C-plane traffic of all UEs is served by the MCBS only. For FCBSs with CUCA, let $\sigma_{\text{MC,cuca,df,s}}$ denote the aggregate capacity of all MUs over M_T RBs for Q TTIs without reusing M_{T} in FCBSs, which is given by,

$$\sigma_{\text{MC,cuca,df,s}} = \left(1-x_{\text{cp}}\right) \times \sum_{t=1}^{Q} \sum_{i=1}^{M_{\text{T}}} \sigma_{t,i}\left(\rho_{t,i}\right) \tag{22}$$

where σ and ρ are responses over M_{T} RBs of all MUs in $t \in \boldsymbol{T}$.

Hence, for FCBSs with CUCA operating at a different frequency mmWave, the overall system capacity of the multi-tier network over M_{T} RBs for all MUs and m_{T} RBs for all FUs per building for Q TTIs can be expressed as the sum throughput of all UEs as follows.

$$\begin{aligned}\sigma_{\mathrm{T,cuca,df,s}} &= \sigma_{\mathrm{MC,cuca,df,s}} + \sigma_{\mathrm{cuca,df,s}} \\ &= \left(1-\varkappa_{\mathrm{cp}}\right)\times\sum_{t=1}^{Q}\sum_{i=1}^{M_{\mathrm{T}}}\sigma_{t,i}\left(\rho_{t,i}\right)+\left(1-\varkappa_{\mathrm{cp}}\right)\times\xi_{\mathrm{t,df}}\times\left(U_{\mathrm{FC}}\times\left(m_{\mathrm{FC}}\times\sigma_{\mathrm{thr,df}}\right)\times Q\right)\end{aligned} \tag{23}$$

For FCBSs with CUSA, the aggregate capacity of all MUs over M_T RBs for Q TTIs is the same as that of CUCA such that

$$\sigma_{\mathrm{MC,cusa,df,s}} = \sigma_{\mathrm{MC,cuca,df,s}} \tag{24}$$

However, since C-plane traffic of all FCBSs with CUSA is served by the MCBS, the aggregate capacity of all FUs at the mmWave band for Q TTIs is given by,

$$\begin{aligned}\sigma_{\mathrm{cusa,df,s}} &= \sigma_{\mathrm{FC,all,df}} \\ &= \xi_{\mathrm{t,df}}\times\left(U_{\mathrm{FC}}\times\left(m_{\mathrm{FC}}\times\sigma_{\mathrm{thr,df}}\right)\times Q\right)\end{aligned} \tag{25}$$

Hence, like CUCA, the overall system capacity of FCBSs with CUSA operating at a different frequency mmWave for Q TTIs can be expressed as

$$\begin{aligned}\sigma_{\mathrm{T,cusa,df,s}} &= \sigma_{\mathrm{MC,cusa,df,s}} + \sigma_{\mathrm{cusa,df,s}} \\ &= \left(1-\varkappa_{\mathrm{cp}}\right)\times\sum_{t=1}^{Q}\sum_{i=1}^{M_{\mathrm{T}}}\sigma_{t,i}\left(\rho_{t,i}\right)+\xi_{\mathrm{t,df}}\times\left(U_{\mathrm{FC}}\times\left(m_{\mathrm{FC}}\times\sigma_{\mathrm{thr,df}}\right)\times Q\right)\end{aligned} \tag{26}$$

B) Single Band Co-Channel Microwave Frequency Enabled FCBSs

Like a single band different frequency mmWave, when FCBSs operate at a single band co-channel microwave frequency, C-plane traffic of all MUs is served by the MCBS and FUs by the FCBSs with CUCA, whereas C-plane traffic of all UEs is served by the MCBS only for FCBSs with CUSA. For FCBSs with CUCA, the aggregate capacity of all MUs for M_T RBs at microwave band for Q TTIs is given by,

$$\sigma_{\mathrm{MC,cuca,cc,s}} = \left(1-\varkappa_{\mathrm{cp}}\right)\times\sum_{t=1}^{Q}\sum_{i=1}^{M_{\mathrm{T}}}\sigma_{t,i}\left(\rho_{t,i}\right) \tag{27}$$

where σ and ρ are responses over M_T RBs of only indoor MUs in $t\in \boldsymbol{T}_{\mathbf{ABS}}$ and all outdoor and offloaded MUs in $t\in \boldsymbol{T}$. Using (8) for $\sigma_{\mathrm{cuca,cc,s}}$, the overall capacity is given by,

$$\begin{aligned}\sigma_{\mathrm{T,cuca,cc,s}} &= \sigma_{\mathrm{MC,cuca,cc,s}} + \sigma_{\mathrm{cuca,cc,s}} \\ &= \left(1-\varkappa_{\mathrm{cp}}\right)\times\sum_{t=1}^{Q}\sum_{i=1}^{M_{\mathrm{T}}}\sigma_{t,i}\left(\rho_{t,i}\right)+\left(1-\varkappa_{\mathrm{cp}}\right)\times\left(1-\phi\right)\times\xi_{\mathrm{t,cc}}\times\left(U_{\mathrm{FC}}\times\left(M_{\mathrm{FC}}\times\sigma_{\mathrm{thr,cc}}\right)\times Q\right)\end{aligned} \tag{28}$$

For FCBSs with CUSA, the aggregate capacity of all MUs for M_T RBs at microwave band for Q TTIs is the same as that of CUCA such that

$$\sigma_{\mathrm{MC,cusa,cc,s}} = \left(1-\varkappa_{\mathrm{cp}}\right)\times\sum_{t=1}^{Q}\sum_{i=1}^{M_{\mathrm{T}}}\sigma_{t,i}\left(\rho_{t,i}\right) \tag{29}$$

Using Eq. (17) for $\sigma_{\mathrm{cusa,cc,s}}$, the overall system capacity is given by,

$$\begin{aligned}\sigma_{\mathrm{T,cusa,cc,s}} &= \sigma_{\mathrm{MC,cusa,cc,s}} + \sigma_{\mathrm{cusa,cc,s}} \\ &= \left(1-\varkappa_{\mathrm{cp}}\right)\times\sum_{t=1}^{Q}\sum_{i=1}^{M_{\mathrm{T}}}\sigma_{t,i}\left(\rho_{t,i}\right)+\left(1-\phi\right)\times\xi_{\mathrm{t,cc}}\times\left(U_{\mathrm{FC}}\times\left(M_{\mathrm{FC}}\times\sigma_{\mathrm{thr,cc}}\right)\times Q\right)\end{aligned} \tag{30}$$

C) Dual Bands Enabled FCBSs

For dual bands enabled FCBSs with CUSA, C-plane traffic of all MUs is served by the MCBS and FUs by the FCBSs at co-channel microwave frequency. The aggregate capacity of all MUs for M_{T} RBs at the microwave band for Q TTIs is given by,

$$\sigma_{\mathrm{MC,cusa,cc,d}} = \left(1 - x_{\mathrm{cp}}\right) \times \sum_{t=1}^{Q} \sum_{i=1}^{M_{\mathrm{T}}} \sigma_{t,i}\left(\rho_{t,i}\right) \tag{31}$$

where σ and ρ are responses over M_{T} RBs of only indoor MUs in $t \in \boldsymbol{T}_{\mathbf{ABS}}$ and all outdoor and offloaded MUs in $t \in \boldsymbol{T}$. Using Eq. (19) for $\sigma_{\mathrm{cusa,df,d}}$, the overall system capacity is given by,

$$\begin{aligned} \sigma_{\mathrm{T,cusa,d}} &= \sigma_{\mathrm{MC,cusa,cc,d}} + \sigma_{\mathrm{cusa,df,d}} \\ &= \left(1 - x_{\mathrm{cp}}\right) \times \sum_{t=1}^{Q} \sum_{i=1}^{M_{\mathrm{T}}} \sigma_{t,i}\left(\rho_{t,i}\right) + \xi_{\mathrm{t,cc}} \times \left(U_{\mathrm{FC}} \times \left(M_{\mathrm{FC}} \times \sigma_{\mathrm{thr,cc}}\right) \times Q\right) \end{aligned} \tag{32}$$

6.3. Energy Efficiency

Energy efficiency is defined as the amount of energy required per bit transmission, which can be expressed as follows for FC networks [33-34].

$$\eta_{\mathrm{ee}} = P_{\mathrm{FC}} / \sigma_{\mathrm{a}} \tag{33}$$

where η_{ee} is the average energy per bit transmission in joules per bit (J/b). $P_{\mathrm{FC}} = 20$ dBm denotes the transmit power of any FCBSs, and σ_{a} denotes the aggregate capacity per TTI for the respective FCBS architectures in the downlink.

6.4. Proportional Fair Scheduling

Since proportional fair scheduler provides an optimal trade-off between fairness and throughput performances, we consider it to schedule time and frequency resources among UEs. Based on the current and past average throughputs of a UE, it schedules a UE $x_i(t)$ in TTI t at RB i with the maximum performance metric given by [35],

$$x_i(t) = \arg\max_{x} \left(\sigma_{x,i}(t) / \tilde{\sigma}_{x,i}(t)\right) \tag{34}$$

where $\sigma_{x,i}(t)$ and $\tilde{\sigma}_{x,i}(t)$ represent respectively the current and past average throughputs of UE x at RB i in TTI t. The past average throughput $\tilde{\sigma}_{x,i}(t)$ at RB i is updated in every TTI as follows [36] where t_{c} denotes adjustable time constant.

$$\tilde{\sigma}_{x,i}(t+1) = \begin{Bmatrix} \tilde{\sigma}_{x,i}(t)\left(1 - 1/t_{\mathrm{c}}\right) + 1/t_{\mathrm{c}}\, \sigma_{x,i}(t), & x = x_i(t) \\ \tilde{\sigma}_{x,i}(t)\left(1 - 1/t_{\mathrm{c}}\right), & x \neq x_i(t) \end{Bmatrix} \tag{35}$$

6.5. Jain's Fairness Index

Jain's fairness index is used to evaluate fairness performance of users served by FCBSs and can be expressed as follows [36-37].

$$F_{\mathrm{J}} = \left(\sum_{x=1}^{U_{\mathrm{F}}} X_x\right)^2 \Bigg/ \left(U_{\mathrm{F}} \times \sum_{x=1}^{U_{\mathrm{F}}} X_x^{\,2}\right) \tag{36}$$

where X_x represents the total number of RBs allocated to user x over the simulation runtime.

DOI:10.4186/ej.2017.21.3.309

7. System Level Resource Scheduling Algorithm and Implementation

A resource scheduling algorithm for FCBSs with CUCA and CUSA to evaluate system level performance is given in Algorithm 2. Frequency-domain schedulers for FCBSs can be implemented either per building basis where all FCBSs in a building can be scheduled or per cluster basis where FCBSs in each cluster in a building can be scheduled by frequency-domain schedulers based on the cluster size. Depending on the architecture of FCBSs, either one or multiple frequency-domain schedulers are needed. For instance, FCBSs enabled with dual bands, i.e. co-channel microwave and mmWave bands, two frequency-domain schedulers, one for microwave and the other for mmWave bands, are required to schedule RBs of respective bands to serve FUs (Fig. 7).

For co-channel microwave enabled FCBSs, in joint scheduler implementations [38], all the frequency-domain schedulers are implemented jointly with the time-domain scheduler, typically located at the MCBS. However, for disjoint scheduler implementations, each frequency-domain scheduler can be implemented at the location of respective buildings or clusters. Any FCBSs within either a building or a cluster as aforementioned can be considered to serve as a frequency-domain scheduler, and is literally termed as cluster head (CH) [38]. A CH allocates RBs to FCBSs during non-ABSs. The time-domain scheduler updates each CH the number of non-ABSs per APP based on the information provided by indoor MUs within a building in the uplink. The presence of an indoor MU during any APPs causes to send information about the ABS pattern for the next APP to the corresponding frequency-domain scheduler via X2 backhauls. However, for joint implementations, frequency-domain schedulers at the MCBS allocate RBs to FCBSs via their respective CHs by sending information over X2 backhauls.

For FCBSs enabled with a different frequency from that of the MCBS and PCBSs, the frequency-domain schedulers can schedule RBs in all TTIs, and are preferable to be implemented at the CH to avoid delay from X2 backhauls. However, for co-channel microwave enabled FCBSs, depending on the small-scale fading effect and backhaul capacity, the choice of frequency-domain scheduler implementations can be made. More specifically, it is preferable to consider dis-joint scheduler implementations to address the small-scale fading effect, whereas joint implementations to minimize delay from X2 backhauls.

Algorithm 2. System level resource scheduling algorithm for FCBSs with CUCA and CUSA

01: **Inputs**:

(i) Set: M_{T} , m_{T} , $\sigma_{\mathrm{thr,se}} = \left\{\sigma_{\mathrm{thr,cc}}, \sigma_{\mathrm{thr,df}}\right\}$, x_{cp} , P_{M}, P_{P}, P_{F}, μ, S_{P}, S_{F}, N, U_{P}, U_{F}, Q, L, ϕ ,

t_{c}, β, G_{t} , G_{r} , L_{F} , $d_{\min}$, $y_{\max,\mathrm{tra}}$, $y_{\max,\mathrm{ter}}$, $\alpha_{\mathrm{f}}(d_{\mathrm{ter}})$, d_{ver}

02: (ii) Initialize: $t \in \{\boldsymbol{T}_{\mathrm{ABS}}, \boldsymbol{T} \setminus \boldsymbol{T}_{\mathrm{ABS}}\} = \{1,\ldots,Q\}$

03: (iii) Estimate: $\forall t,i : \left\{PL_{t,i}, LS_{t,i}, SS_{t,i}, \rho_{t,i}, \sigma_{t,i}\left(\rho_{t,i}\right)\right\}$, U_{FC} , M_{FC} , m_{FC} , σ_{a} , $\xi_{\mathrm{t,cc}}$, $\xi_{\mathrm{t,df}}$

04: // *Intra-and inter-floor interference estimation*

05: Estimate: $\forall d_{\mathrm{tra}}\ \alpha_{\mathrm{tra}}\left(d_{\mathrm{tra}}\right) = \left(d_{\min}/d_{\mathrm{tra}}\right)^3$

06: $\forall d_{\mathrm{ter}}\ \alpha_{\mathrm{ter}}\left(d_{\mathrm{ter}}\right) = 10^{-(0.1\alpha_{\mathrm{f}}(d_{\mathrm{ter}}))}\left(d_{\min}/d_{\mathrm{ter}}\right)^3$

07: // *RoE estimation*

08: Estimate: $\forall \sigma_{\mathrm{thr,se}}\ d_{\mathrm{tra}}^{*} \geq d_{\min}\left(y_{\max,\mathrm{tra}}\left(2^{\sigma_{\mathrm{thr,se}}}-1\right)\right)^{1/3}$

09: $\forall \sigma_{\mathrm{thr,se}}\ d_{\mathrm{ter}}^{*} \geq d_{\min}\left(10^{-\left(0.1\alpha_{\mathrm{f}}\left(d_{\mathrm{ter}}^{*}\right)\right)}\ y_{\max,\mathrm{ter}}\left(2^{\sigma_{\mathrm{thr,se}}}-1\right)\right)^{1/3}$

10: // *Capacity estimation*

11: Estimate (capacity of all FUs for all FCBS architectures):

12: $\sigma_{\mathrm{cuca,cc,s}} = \left(1-x_{\mathrm{cp}}\right)\times\left(1-\phi\right)\times\xi_{\mathrm{t,cc}}\times\left(U_{\mathrm{FC}}\times\left(M_{\mathrm{FC}}\times\sigma_{\mathrm{thr,cc}}\right)\times Q\right)$

13: $\sigma_{\mathrm{cuca,df,s}} = \left(1-x_{\mathrm{cp}}\right)\times\xi_{\mathrm{t,df}}\times\left(U_{\mathrm{FC}}\times\left(m_{\mathrm{FC}}\times\sigma_{\mathrm{thr,df}}\right)\times Q\right)$

14: $\sigma_{\mathrm{cusa,cc,s}} = = \left(1-\phi\right)\times\xi_{\mathrm{t,cc}}\times\left(U_{\mathrm{FC}}\times\left(M_{\mathrm{FC}}\times\sigma_{\mathrm{thr,cc}}\right)\times Q\right)$

15: $\sigma_{\text{cusa,df,s}} = \xi_{\text{t,df}} \times \left(U_{\text{FC}} \times \left(m_{\text{FC}} \times \sigma_{\text{thr,df}} \right) \times Q \right)$

16: $\sigma_{\text{cusa,df,d}} = \xi_{\text{t,df}} \times \left(U_{\text{FC}} \times \left(m_{\text{FC}} \times \sigma_{\text{thr,df}} \right) \times Q \right)$

17: Estimate (capacity of all MUs for all FCBS architectures):

18: $\forall U_{\text{MI}} \forall t \in \boldsymbol{T}_{\text{ABS}} \ \wedge \forall U_{\text{MP}} \forall t \in \boldsymbol{T} \ \ \sigma_{\text{MC,cuca,cc,s}} = \left(1 - \varkappa_{\text{cp}}\right) \times \sum_{t=1}^{Q} \sum_{i=1}^{M_{\text{T}}} \sigma_{t,i} \left(\rho_{t,i} \right)$

19: $\forall t \in \boldsymbol{T} \ \ \sigma_{\text{MC,cuca,df,s}} = \left(1 - \varkappa_{\text{cp}}\right) \times \sum_{t=1}^{Q} \sum_{i=1}^{M_{\text{T}}} \sigma_{t,i} \left(\rho_{t,i} \right)$

20: $\forall U_{\text{MI}} \forall t \in \boldsymbol{T}_{\text{ABS}} \ \wedge \forall U_{\text{MP}} \forall t \in \boldsymbol{T} \ \ \sigma_{\text{MC,cusa,cc,s}} = \left(1 - \varkappa_{\text{cp}}\right) \times \sum_{t=1}^{Q} \sum_{i=1}^{M_{\text{T}}} \sigma_{t,i} \left(\rho_{t,i} \right)$

21: $\forall t \in \boldsymbol{T} \ \ \sigma_{\text{MC,cusa,df,s}} = \left(1 - \varkappa_{\text{cp}}\right) \times \sum_{t=1}^{Q} \sum_{i=1}^{M_{\text{T}}} \sigma_{t,i} \left(\rho_{t,i} \right)$

22: $\forall U_{\text{MI}} \forall t \in \boldsymbol{T}_{\text{ABS}} \ \wedge \forall U_{\text{MP}} \forall t \in \boldsymbol{T} \ \ \sigma_{\text{MC,cusa,cc,d}} = \left(1 - \varkappa_{\text{cp}}\right) \times \sum_{t=1}^{Q} \sum_{i=1}^{M_{\text{T}}} \sigma_{t,i} \left(\rho_{t,i} \right)$

23: Estimate (overall system capacity for all FCBS architectures):

24: $\sigma_{\text{T,cuca,cc,s}} = \sigma_{\text{MC,cuca,cc,s}} + \sigma_{\text{cuca,cc,s}}$

25: $\sigma_{\text{T,cuca,df,s}} = \sigma_{\text{MC,cuca,df,s}} + \sigma_{\text{cuca,df,s}}$

26: $\sigma_{\text{T,cusa,cc,s}} = \sigma_{\text{MC,cusa,cc,s}} + \sigma_{\text{cusa,cc,s}}$

27: $\sigma_{\text{T,cusa,df,s}} = \sigma_{\text{MC,cusa,df,s}} + \sigma_{\text{cusa,df,s}}$

28: $\sigma_{\text{T,cusa,d}} = \sigma_{\text{MC,cusa,cc,d}} + \sigma_{\text{cusa,df,d}}$

29: Estimate (energy efficiency of all FUs for all FCBS architectures):

30: $\forall \sigma_{\text{a}} \ \eta_{\text{ee}} = P_{\text{FC}} / \sigma_{\text{a}}$

31: Estimate (Jain's fairness index for FC networks):

32: $F_{\text{J}} = \left(\sum_{x=1}^{U_{\text{F}}} X_x \right)^2 \Big/ \left(U_{\text{F}} \sum_{x=1}^{U_{\text{F}}} X_x^{\ 2} \right)$

33: **Outputs**:

34: Display: d_{tra}^{*}, d_{ter}^{*}, U_{FC}, M_{FC}, m_{FC}, $\xi_{\text{t,cc}}$, $\xi_{\text{t,df}}$, F_{J}

35: Plot: $\eta_{\text{ee}}, \sigma_{\text{T,cuca,cc,s}}, \sigma_{\text{MC,cuca,cc,s}}, \sigma_{\text{cuca,cc,s}}, \sigma_{\text{T,cuca,df,s}}, \sigma_{\text{MC,cuca,df,s}}, \sigma_{\text{cuca,df,s}},$
$\sigma_{\text{T,cusa,cc,s}}, \sigma_{\text{MC,cusa,cc,s}}, \sigma_{\text{cusa,cc,s}}, \sigma_{\text{T,cusa,df,s}}, \sigma_{\text{MC,cusa,df,s}}, \sigma_{\text{cusa,df,s}},$
$\sigma_{\text{T,cusa,d}}, \sigma_{\text{MC,cusa,cc,d}}, \sigma_{\text{cusa,df,d}}$

8. Simulation Parameters, Assumptions, and Performance Results

8.1. Simulation Parameters and Assumptions

The default simulation parameters and assumptions used for the system level simulation are listed in Table 3. Unless stated explicitly, the default value for any parameters is used from Table 3. Note that we consider empirical simplified path loss model for indoor FCs and assume the similar mechanisms for the dual-strip model for evaluating the performance of FCs [27] recommended by the 3GPP. We consider that FCs in all buildings experience the similar signal propagation characteristics. Hence, there would not be any significant deviation in the performance results from using empirical models that do not necessarily guarantee the transportability between environments. Since in digital cellular mobile systems, information is transmitted in every discrete transmission time interval (TTI), e.g. 1 ms for long-term evolution-advanced (LTE-Advanced) mobile systems, we consider the discrete-event type simulation at TTI of 1 ms to execute simulation results. Further, for evaluating the performances by simulation and solving the formulated optimization problems, the computational tool MATLAB Release 2013a is used.

DOI:10.4186/ej.2017.21.3.309

8.2. Performance Results

8.2.1. Performance evaluation

From Eq. (1) and Eq. (2), the aggregate interferences in both intra-and inter-floor levels at a sFU is inversely related to the required minimum distances d^*_{tra} and d^*_{ter} respectively. Further, because of an additional floor attenuation effect $10^{-(0.1\alpha_{\text{f}}(d_{\text{ter}}))}$, the inter-floor interference power decays considerably faster with distance as compared to the intra-floor interference power. Hence, floor penetration losses play a significant role on inter-floor interference effect at a sFU. We consider link spectral efficiencies of 3.459 bps/Hz and 3.9 bps/Hz, which are corresponding to the aggregate interferences experienced by the desired link between a sFU and a sFCBS, when operating at a co-channel microwave and a different frequency mmWave bands respectively. This is because, typically mmWave bands have better link quality than that of microwave bands. Hence, $\sigma_{\text{thr,cc}} = 3.459$ bps/Hz and $\sigma_{\text{thr,df}} = 3.9$ bps/Hz are chosen such that the cluster sizes of FCBSs when operating at both bands are the same. Further, for the time-domain eICIC, ABS=1 is considered.

Using Eq. (3), for link spectral efficiencies of 3.459 bps/Hz and 3.9 bps/Hz, the corresponding minimum distances must be equal or greater than 22 m and 24 m respectively in intra-floor level. Since these values of distance are less than 25 m, resources can be reused in FCBSs in intra-floor level that are two-tier apart. Similarly using Eq. (4), for link spectral efficiencies of 3.459 bps/Hz and 3.9 bps/Hz, the corresponding minimum distances in inter-floor level must be equal or greater than 2 m and 2.9 m respectively. Because these values of distance are less than 3 m of a floor's height, resources can be reused in every floor in a building.

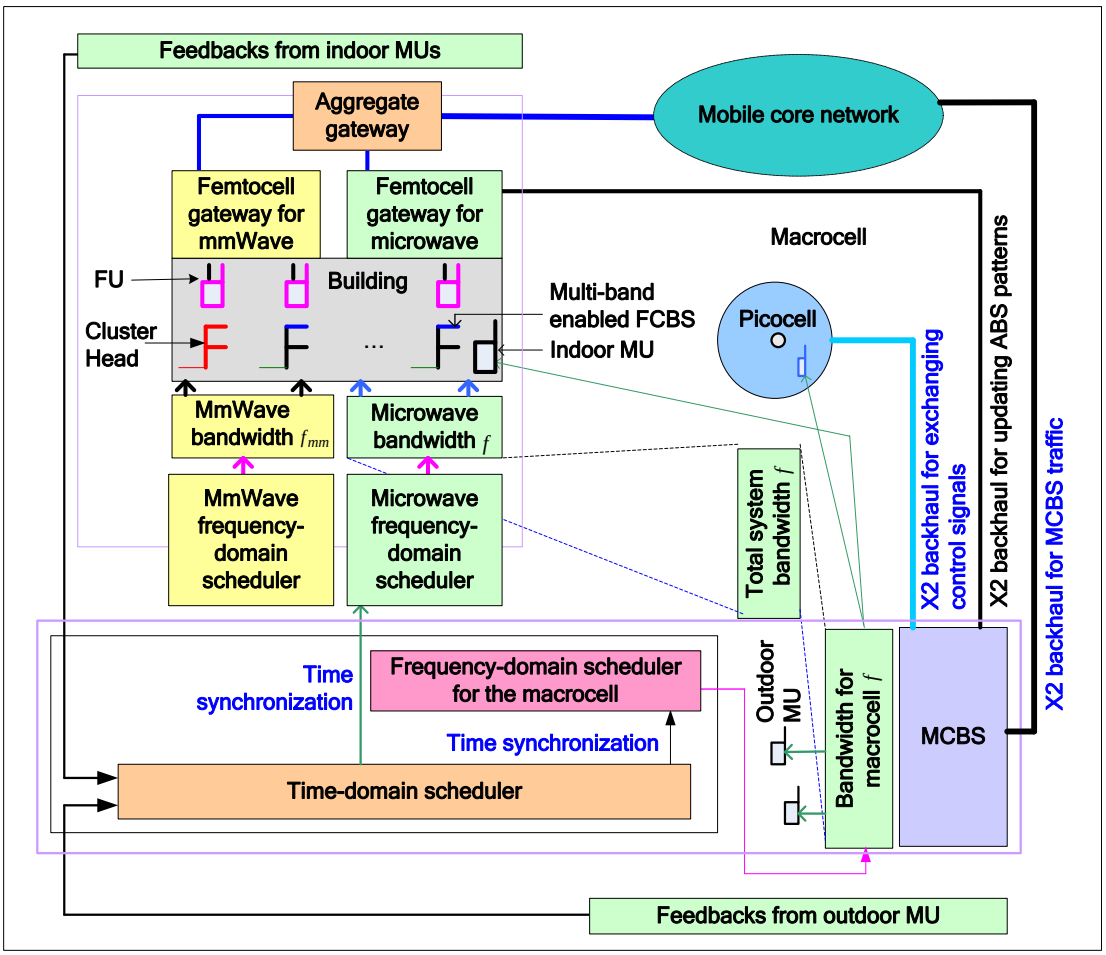

Fig. 7. Disjoint frequency-domain scheduler implementations for dual bands enabled FCBSs per cluster basis.

Table 3. Default simulation parameters and assumptions.

Parameters and Assumptions			Value
E-UTRA simulation case[1]			3GPP case 3
Cellular layout[2] and Inter-site distance (ISD)[1,2]			Hexagonal grid, dense urban, 3 sectors per MC site and 1732 m
Carrier frequency[2,3] and transmit direction			2 GHz (microwave), 60 GHz (mmWave line-of-sight) and downlink
System bandwidth			5 MHz (for both 2 GHz and 60 GHz)
Number of cells			1 MC, 2 PCs, and 250 FCs
Total BS transmit power[1] (dBm)			46 for MC[1,6], 37 for PC[1], 20 (for 2 GHz) for FC[1,3,6] and 17.3 (for 60 GHz) for FC[1,3]
Co-channel fading model[1]			Frequency selective Rayleigh for MC and PC and Rician for FC
External wall penetration loss[1] (L_{ow})			20 dB
Path loss	MCBS and a UE[1]	Outdoor MU	PL(dB)=15.3 + 37.6log$_{10}R$, R is in m
		Indoor MU	PL(dB)=15.3 + 37.6log$_{10}R$ + L_{ow}, R is in m
	PCBS and a UE[1]		PL(dB)=140.7+36.7log$_{10}R$, R is in km
	FCBS and a UE[1,2,3]		PL(dB)=127+30log$_{10}$(R/1000) for 2 GHz; PL(dB) = 68+21.7log$_{10}$(R) for 60 GHz, R is in m
Lognormal shadowing standard deviation (dB)			8 for MCBS[2] , 10 for PCBS[1], 10 (for 2 GHz) and 0.88 (for 60 GHz) for FCBS[2,3]
Antenna configuration			Single-input single-output for all BSs and UEs
Antenna pattern (horizontal)			Directional (120^0) for MC[1] and omnidirectional for PC[1] and FC[1]
Antenna gain plus connector loss (dBi)			14 for MCBS[2], 5 for PCBS[1], 5 (for 2 GHz) and 5 (for 60 GHz, Biconical horn) for FCBS[1,3]
UE antenna gain[2,3]			0 dBi (for 2 GHz), 5 dBi (for 60 GHz, Biconical horn)
UE noise figure[2,4] and UE speed[1]			9 dB, 3 km/hr
Total number of MUs and number of UEs per FC			30 and 1
PC coverage and MUs offloaded to all PCs[1]			40 m (radius), 2/15
Indoor MUs[1]			35%
3D multi-storage building and FC models (regular square-grid)		Number of buildings	1
		Number of floors per building	10
		Number of apartments per floor	25
		Number of FCBSs per apartment	1
		FCBS activation ratio	100%
		FCBS deployment ratio	1
		Total number of FCBSs per building	250
		Area of an apartment	$10\times10\,m^2$
		Location of a FCBS in an apartment	Center
		d_{min}[5] and d_{ver}[5]	5 m and 3 m
		$y_{max,tra}$[5]	8
		$y_{max,ter}$[5] Single-sided cFCBSs	1
		$y_{max,ter}$[5] Double-sided cFCBSs	2
Scheduler and traffic model[2]			Proportional Fair and full buffer
Type of FCs			Closed subscriber group
Channel state information			Ideal
Spectral efficiency constraints for FCBSs			3.459 bps/Hz for microwave and 3.9 bps/Hz for mmWave
TTI[1] and scheduler time constant (t_c)			1 ms and 100 ms
ABS pattern, APP, and total simulation run time			1/8, 8 ms, and 8 ms

Note: Taken [1]from [39] , [2]from [27], [3]from [40], [4]from [41], [5][26], and [6][43].

Using expressions for capacity estimations in section 6, the aggregate capacity responses of various FCBSs architectures as discussed in section 2 are shown Fig. 8. Note that with the term capacity, we implicitly represent U-plane data traffic capacity of UEs. From Fig. 8, it can be found that most data traffic is served by FCBSs as compared to the MCBS and PCBSs. Further, FCBSs with CUSA serve more traffic than with CUCA irrespective of the type of frequency bands and the number of transceivers at any FCBSs. Likewise, FCBSs operating at the mmWave band serve more traffic than operating at the co-channel microwave band because of better link quality at mmWave band between a FU and a FCBS.

Since in dual bands enabled FCBSs, only the mmWave band serves U-plane traffic, the overall system capacities obtained from a single transceiver and a dual transceivers based FCBSs are the same. However, dual transceivers based FCBSs gain advantages from the reduced control signaling overhead because of no cooperation needed between the C-plane and U-plane BSs. Besides, when a single transceiver based FCBS operates at the mmWave band, no CCI coordination is needed between the MUs and FUs. Hence, the aggregate capacity of all MUs increases, as shown in Fig 8.

Figure 9 shows the energy efficiency performances of FCBSs with CUCA and CUSA. As aforementioned, because FCBSs with CUSA can serve more traffic (Fig. 8) for the same bandwidth than with CUCA, the energy required per bit transmission of FCBSs with CUSA is correspondingly less than FCBSs with CUCA in the downlink. Overall, among all FCBS architectures discussed in section 2, a single transceiver co-channel microwave enabled FCBSs with CUCA provides the worse, and a single or dual transceivers mmWave enabled FCBSs with CUSA provides the best overall system capacity and average FC networks' energy efficiency performances.

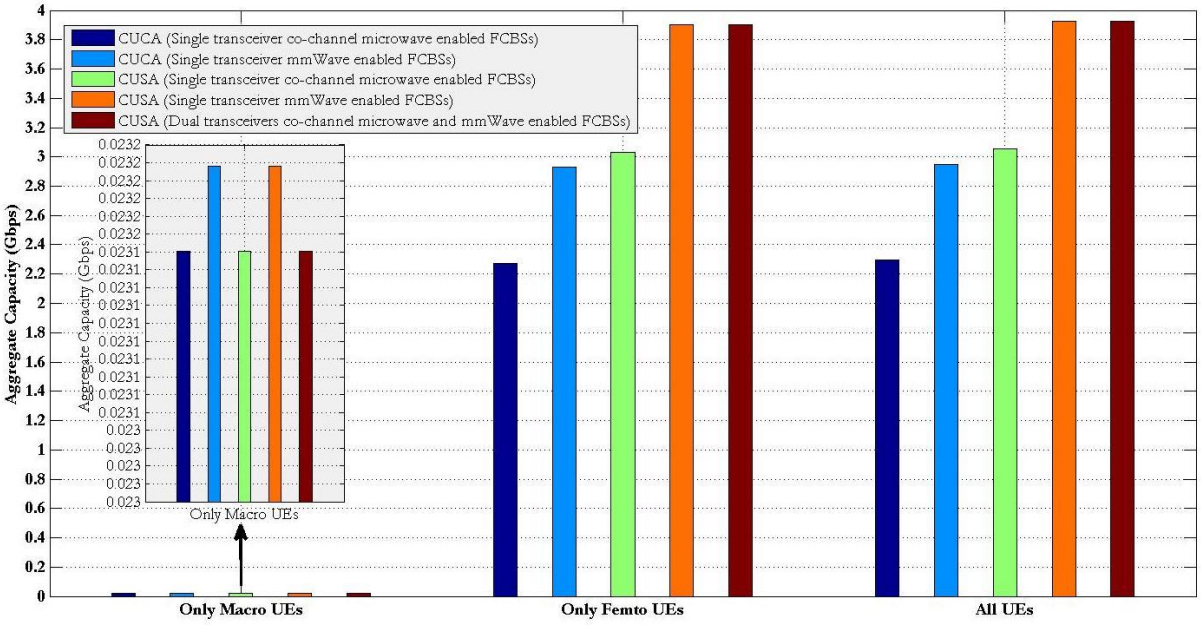

Fig. 8. Capacity performances of FCBSs with CUCA and CUSA.

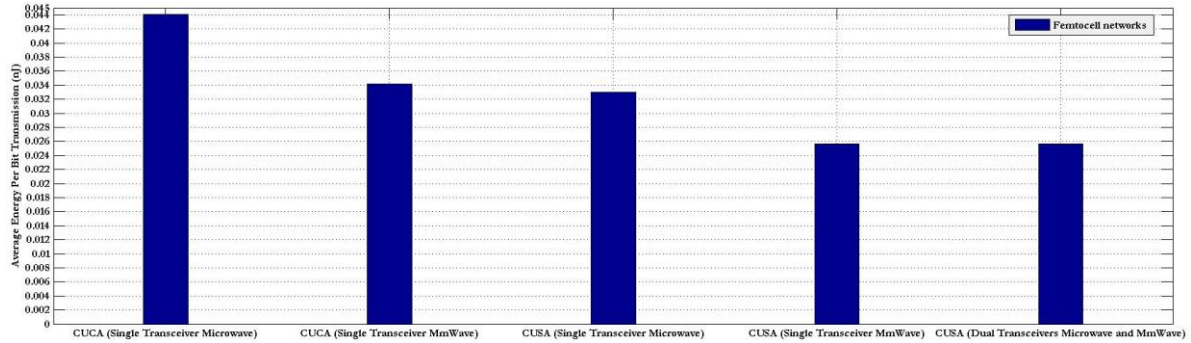

Fig. 9. Energy efficiency performances of FCBSs with CUCA and CUSA.

8.2.2. Performance comparison

To evaluate the performances of the proposed resource reuse approach, we consider the resource reuse approach proposed in [26] to compare in terms of the capacity and fairness performances. We consider the total capacity of both C-/U-plane of all UEs in the system for a non-ABS for FCBSs with CUCA under the same scenario (i.e., more specifically, reused frequency resources of 5 MHz, a link spectral efficiency constraint $\sigma_{\text{thr,se}} = 3.459$ bps/Hz for microwave frequency, a building having 10 floors, and each floor with 25 apartments). Each apartment has one FCBS, and each FCBS serves only one UE.

Hence using Eq. (28), for a single band co-channel microwave frequency, an average system capacity of 286.85 Mbps per TTI can be achieved with our proposed resource reuse approach. This is considerably greater than the achievable system capacity of 135 Mbps per TTI for non-orthogonal resource reuse and allocation by the resource reuse approach proposed in [26] for the number of reused RBs of 5 per cFCBS. Though in [26], with an increase in reused RBs per cFCBS from 5 to 10, the achievable capacity increases near proportionally, the increased capacity is still less than what can be achieved by our proposed resource reuse approach. Moreover, with an increase in reused RBs from 5 to 10, the fairness factor degrades significantly from 0.087 for 5 RBs to 0.062 for 10 RBs [26] because of competing relatively more by non-cFCBSs with a reduced number of RBs allocated for them. Furthermore, it is unusual to allocate 40% of the total system bandwidth to a cFCBS and is not recommendable too in order to ensure the quality of service for non-cFCBSs. On the contrary, in our proposed resource reuse approach, each FCBS within a cluster is assigned statically an equal amount of bandwidth, and therefore the fairness factor for resource allocations among all cFCBSs is 1. Hence, our proposed resource reuse approach performs better than that proposed in [26] in terms of both the system capacity as well as fairness in resource allocations among all FCBSs with CUCA in a building as shown in Fig. 10 where the all capacity values are normalized with respect to the capacity achieved by our proposed resource reuse approach.

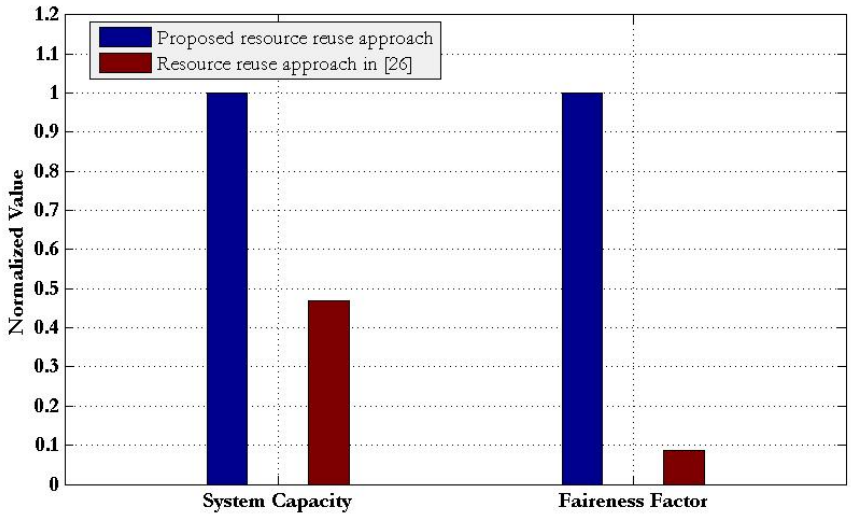

Fig. 10. System capacity and fairness performances of FCBSs with CUCA with the proposed resource reuse approach and the resource reuse approach in [26] for *L*=1 per TTI.

9. Features, Issues, and Applications of FCBSs with CUCA and CUSA

9.1. Features and Issues

Operating a FCBS with CUCA benefits from a reduced or no control signaling overhead for the cooperation of C-/U-plane BSs and suffers from achieving a high data rate in indoor. On the contrary, when operating with CUSA, a single band enabled FCBS can achieve a high data rate in indoor but suffer from originating a considerable amount of control signaling overhead for the cooperation of C-/U-plane BSs. In Table 4, we point out major features and issues of FCBSs with CUCA and CUSA as shown in Fig. 2.

Table 4. Features and issues of FCBSs with CUCA and CUSA.

Feature and Issue	FCBSs with CUCA	FCBSs with CUSA
Strength and weakness	Low resource utilization	High resource utilization
	No U-plane cell discovery mechanism is needed	U-plane cell discovery mechanism is needed particularly for single band enabled FCBSs
	Low U-plane data traffic capacity of FCBSs because of allocating a certain portion of the bandwidth to C-plane traffic	High U-plane data traffic capacity of FCBSs since C-plane traffic is served by the MCBS so that all resources can be allocated to serve U-plane traffic of FCBSs
	No cooperation between the MCBS and FCBSs is not needed for C-plane traffic	Cooperation between the MCBS and FCBSs is a must for C-plane traffic to make aligned with U-plane traffic for a single band enabled FCBSs
	The transmit power of the MCBS and FCBSs is always on and hence low system level energy efficiency	The transmit power of the MCBS is always on, whereas the transmit power of FCBSs to serve U-plane traffic is switched on based on the UE generated traffic requests, and hence a high system level energy efficiency can be achieved
	Control signaling network is simple	Control signaling network is complex, particularly for a single band enabled FCBSs
	No feedback signaling delay from switching FCBSs	Considerable feedback signaling delay from switching the transmit power of FCBSs between on and off states
Viability challenge	Because of coupled C-/U-plane, network management is complex	The signaling network is complicated, particularly for a single band enabled FCBSs
	Because of complex interference and mobility management, the densification of FCBSs to enhance network capacity is difficult	The FCBS discovery and wake up mechanisms to address energy efficiency are complex, particularly for a single band enabled FCBSs
Open research issue	• Improvement in overall network capacity, spectral efficiency, and energy efficiency • Scaling SCBS densifications with traffic demands • Increase in per user data rate, and simplification of network management	• Simple control signaling network • FCBS discovery and wake up mechanisms • UE association and handover mechanisms • For multi-transceiver based FCBSs, multi-band integration and simultaneous operation and multi-band transceivers design • UE design to avoid self-interference from multiple bands • CCI management when a FCBS is operating at the same band as that of the MCBS

9.2. Applications

In the following, we discuss on the applicability of a multi-band enabled FCBS in contrast to a single band enabled FCBS in light with the prospective device-centric network architectures to split C-/U-plane as well as uplink and downlink (UL/DL) traffic and non-uniform and asymmetric traffic for 5G mobile networks.

9.2.1. Split Architecture

Splitting UL/DL and C-/U-plane is considered as one of the major enabling technologies for 5G mobile networks to address issues such as high energy and spectral efficiencies and high data rate services. To split C-/U-plane and UL/DL, the applicability of a multi-band enabled FCBS architecture is shown in Fig. 2(e) where a FU can communicate with its associated closed subscriber group (CSG) FCBS at co-channel microwave (f_1) for uplink (UL) and/or C-plane traffic and at mmWave (f_2) for downlink (DL) and/or U-

plane traffic by employing dual connectivity features with the same FCBS, as opposed to communicating via different BSs enabled with a single transceiver. A number of variations of this split architecture can be obtained depending on how UL/DL and C-/U-plane traffic are configured for routing through mmWave and microwave bands. For example, co-channel microwave to serve UL traffic and mmWave to serve DL traffic can be completely dedicated. Similarly, C-plane traffic can be served only by the co-channel microwave band and U-plane traffic only by an mmWave band. Note that a UE has to be able to operate at both bands when it is within the coverage, and only at the microwave band when it is out of coverage of its associated CSG FCBS. Since the propagation characteristic over an mmWave band differs considerably from a microwave band, a separate transceiver with a separate baseband unit for each of these bands is needed for the architecture of a UE [38].

C-/U-plane splitting benefits from the multi-band enabled FCBS architecture for issues as follows.

1. Sending a high traffic volume and achieving a high data rate demand of U-plane can be accomplished using the mmWave band via S1 interface directly to the mobile core network [1].
2. By transmitting C-plane traffic at the microwave band, a continuity in connection of a UE between indoor and outdoor environments can be provided resulting less network wide call-drop.
3. By performing baseband processing for U-plane traffic at the CHs in a decentralized manner [1], the conventional centralized U-plane traffic processing at the MCBS can be overcome to allow the density of SCs independent of the centralized baseband processing in order to achieve the high data traffic demand of 5G networks.

UL/DL splitting also benefits from the multi-band enabled FCBS architecture. UL traffic is suited to transmit at the microwave band for such reasons as follows.

1. A microwave signal has less penetration loss and shadowing effect than an mmWave signal and hence helps improve SINR at a FCBS for a UE.
2. UL generated traffic is typically less than that in DL which can be sufficient to be served by the microwave band.

Similarly, DL is suited to transmit at an mmWave band for such reasons as follows.

1. The presence of line-of-sight components of a DL signal at an mmWave band results in a high SINR and throughput per FU.
2. Because of high penetration loss and good channel condition at an mmWave band, high data rate demands in DL can be provided with a small coverage and a low transmit power, which help further increase the SC density.

Overall, since the traffic demand in UL/DL or C-/U-plane is asymmetric, using BS idle mode capability [42] and splitting UL/DL and C-/U-plane by employing the multi-band enabled FCBS architecture, an optimization of FCBS transmit power to address energy efficiency of 5G mobile networks can be achieved.

9.2.2. Non-uniform traffic

Though the average traffic demand has been increased by manifold in the last decade, traffic is not generated uniformly network wide [38] because of such issues as follows.

1. BSs located in urban areas serve more traffic than those in suburban or rural areas.
2. In urban environments, all places are not populated uniformly, e.g. bus stations and shopping malls are more likely to be populated than other places. BSs located in these areas need to serve more traffic than others.
3. The demand for high data rate services is not uniform since the traffic demand largely depends on user profiles, and user characteristics. Hence, it is more probable that a user of upper class residential zones can afford and hence generate more high data rate services than others. Accordingly, more BSs should be installed in such areas.

4. The traffic demand varies with time, e.g. most corporate traffic is generated during 8:00-18:00, whereas most residential traffic is generated during 17:00-23:00.

Since both spectrum band and bandwidth have direct impacts on the capacity, a FCBS implemented with dual spectrums such as microwave and mmWave as shown in Fig. 2(e) can address such non-uniformity in traffic demand as aforementioned. Since an mmWave band provides more capacity than a co-channel microwave band, a multi-band enabled FCBS can be operated at an mmWave spectrum during a high traffic demand and at a co-channel microwave spectrum during a low traffic demand in places where the traffic fluctuation is very high. In both cases, the other off-service transceiver, i.e. co-channel microwave for a high traffic and mmWave for a low traffic, can be switched off to save energy. If necessary, both spectrums can operate at the same time to provide even higher data rate than that when operating at a single spectrum. With such an adaptive multi-spectrum availability in FCBSs, network operators can provide on-demand data rate services, optimize location specific resource allocation, and maximize profit margin.

10. Conclusion

We present in this paper various FCBS architectures for serving C-/U-plane traffic based on the number of transceivers, i.e. single or multiple, and their operating frequency bands. To avoid cost from licensing a new band, we consider reusing the same microwave band of the large MC fully in FCBSs deployed within multi-storage buildings. The cross-tier co-channel interferences between MUs and FUs are avoided using the almost blank subframe (ABS) based enhanced intercell interference coordination. For a different and diverse frequency characteristic, a high frequency mmWave band is considered for FCBSs only. We consider a single transceiver operating at either the co-channel microwave or mmWave band, and for multiple transceivers, dual transceivers are considered operating at both the co-channel microwave and mmWave bands. For reusing resources, the clustering of FCBSs is done using the analytical model proposed in [26]. We propose a static frequency resource reuse approach and develop an algorithm to reuse resources in FCBSs deployed in a multi-storage building having a number of floors, each with 5×5 square-grid apartments, and one FCBS per apartment. For a system level performance evaluation, using the proposed resource reuse approach for FCBSs with CUCA and CUSA, we formulate necessary expressions, develop a resource scheduling algorithm, and discuss the implementation of the resource scheduler.

With a system level simulation, we evaluate the performances of numerous C-/U-plane coupled and separation FCBS architectures in terms of the system capacity and energy efficiency with a multi-tier network consisting a MC, a number of outdoor picocells and indoor FCBSs in multi-storage buildings. It is shown that FCBSs with CUSA serves more traffic than with CUCA irrespective of the type of frequency bands and the number of transceivers at any FCBSs, and hence the energy required per bit transmission for FCBSs with CUSA is corresponding less than that with CUCA. Overall, among all FCBS architectures, a single transceiver co-channel microwave enabled FCBS with CUCA provides the worse and a single or dual transceivers mmWave enabled FCBS with CUSA provides the best overall system capacity and an average FC networks' energy efficiency performances. For a given link quality constraint between a FCBS and a UE and the number of FCBSs in a building, we also demonstrate that our proposed resource reuse approach performs better than that proposed in [26] in terms of both the system capacity as well as fairness in resource allocations among FCBSs with CUCA. Finally, we discuss on the applicability of a multi-band enabled FCBS in contrast to a single band enabled FCBS architecture, and point out a number of features and issues of FCBSs with CUCA and CUSA.

Acknowledgements

The initial results of this paper were presented partly in conference articles [4], [6], and [38]. The research grant funds have been provided by "The 100th Anniversary Chulalongkorn University Fund for Doctoral Scholarship" upon submission of application of research expenses for "The 90th Anniversary Chulalongkorn University Fund (Ratchadaphiseksomphot Endowment Fund)" and "The Electrical Engineering Chulalongkorn University PhD (EECU-PhD) Honors Program Scholarship" at Chulalongkorn University, Bangkok, Thailand. The research is also graciously supported by the STAR Project, Department of Electrical Engineering, Chulalongkorn University, Thailand.

References

[1] H. Ishii, Y. Kishiyama, and H. Takahashi, "A novel architecture for LTE-B: C-plane/U-plane split and phantom cell concept," in *Proc. 2012 IEEE Globecom Workshops*, Anaheim, CA, 3-7 Dec. 2012, pp. 624-630.

[2] H. A. U. Mustafa, M. A. Imran, M. Z. Shakir, A. Imran, and R. Tafazolli, "Separation framework: an enabler for cooperative and D2D communication for future 5G networks," *IEEE Communn. Surveys & Tuts.*, vol. 18, no. 1, pp. 419-445, 2016.

[3] A. Mohamed, O. Onireti, M. A. Imran, A. Imran, and R. Tafazolli, "Control-data separation architecture for cellular radio access networks: a survey and outlook," *IEEE Communn. Surveys & Tuts.*, vol. 18, no. 1, pp. 446-465, 2016.

[4] R. K. Saha and C. Aswakul, "Capacity analysis of control-/user-plane traffic of different small cell base station architectures for 5G cellular," in *Proc. 2017 International Conference on Electronics, Information, and communication (ICEIC),* (to appear in IEEE Xplore), Phuket, Thailand, 11-14 Jan. 2017, pp. 534-537.

[5] F. Boccardi, R. W. Heath Jr., A. Lozano, T. L. Marzetta, and P. Popovski, "Five disruptive technology directions for 5G," *IEEE Commun. Mag.,* vol. 52, no. 2, pp.74-80, Feb. 2014.

[6] R. K. Saha and C. Aswakul, "A novel clustering, frequency reuse and allocation technique for 2D regular grid-based dense urban femtocell deployment for 5G mobile networks," in *Proc. 2017 International Conference on Electronics, Information, and communication (ICEIC),* (to appear in IEEE Xplore), Phuket, Thailand, 11-14 Jan. 2017, pp. 220-223.

[7] A. Capone, A. Fonseca dos Santos, I. Filippini, and B. Gloss, "Looking beyond green cellular networks," in *Proc. 2012 9th Annual Conference on Wireless On-Demand Network Systems and Services (WONS)*, 9-11, 2012, pp. 127-130.

[8] X. Xu, G. He, S. Zhang, Y. Chen, and S. Xu, "On functionality separation for green mobile networks: concept study over LTE," *IEEE Commun. Mag.*, vol. 51, no. 5, pp. 82-90, May 2013.

[9] R. K. Saha and C. Aswakul, "Incentive and architecture of multi-band enabled small cell and UE for up-/down-link and control-/user-plane splitting for 5G mobile networks," *Frequenz J. RF-Eng. & Telecommun.,* vol. 71, no. 1-2, pp. 95-118, Jan. 2017.

[10] S. Nagata, K. Takeda, and H. Takahashi, "LTE-Advanced release 12 standardization technology overview," *NTT DOCOMO Tech. J.,* vol. 17, no. 2, pp. 31-35, 2015.

[11] R. Langar, S. Secci , R. Boutaba, and G. Pujolle, "An operations research game approach for resource and power allocation in cooperative femtocell networks," *IEEE Trans. Mob. Comput.,* vol. 14, no. 4, pp. 675-687, Apr. 2015.

[12] N. Saquib, E. Hossain, and D. Kim, "Fractional frequency reuse for interference management in LTE-Advanced hetnets," *IEEE Wireless Commun.* vol. 20, no. 2, pp. 113-122, Apr. 2013.

[13] S. J. Kao and H. L. Wang, "Dynamic orthogonal frequency division multiple access resource management for downlink interference avoidance in two-tier networks," *Int. J. Commun. Syst.,* vol. 28, no. 2, pp. 281-295, Jan. 2015.

[14] C. Bouras, G. Diles, V. Kokkinos, and A. Papazois, "Transmission optimizing on dense femtocell deployments in 5G," *Int. J. Commun. Syst.,* vol. 29, no. 16, pp. 2388-2402, Nov. 2016.

[15] S. Cho and W. Choi, "Coverage and load balancing in heterogeneous cellular networks with minimum cell separation," *IEEE Trans. Mob. Comput.,* vol. 13, no. 9, pp. 1955-1966, Sep. 2014.

[16] S. Cho and W. Choi, "Energy-efficient repulsive cell planning for heterogeneous cellular networks," *IEEE Journal on Selected Areas in Commun.,* vol. 31, no. 5, pp. 870-882, May 2013.

[17] W. Li, W. Zheng, W. Xiangming, and T. Su, "Dynamic clustering based sub-band allocation in dense femtocell environments," in *Proc. 2012 IEEE 75th Vehicular Technology Conference(VTC-Spring)*, 6-9 May 2012, pp. 1-5.

[18] A. Hatoum, R. Langar, N. Ait Saadi, R. Boutaba, and G. Pujolle, "QoS-based power control and resource allocation in OFDMA femtocell networks," in *Proc. IEEE Global Communications Conference (GLOBECOM)*, 3-7 Dec. 2012, pp. 5116-5122.

[19] K. Hosseini, H. Dahrouj, and R. Adve, "Distributed clustering and interference management in two-tier networks," in *Proc. 2012 IEEE Global Communications Conference (GLOBECOM)*, 3-7 Dec. 2012, pp. 4267-4272.

[20] A. Abdelnasser and E. Hossain, "Joint subchannel and power allocation in two-tier OFDMA hetnets with clustered femtocells," in *Proc. 2013 IEEE International Conference on Communications (ICC) Workshops*, pp. 6002-6007, 9-13 June 2013.
[21] A. Abdelnasser and E. Hossain, "Subchannel and power allocation schemes for clustered femtocells in two-tier OFDMA hetnets", in *Proc. 2013 IEEE International Conference on Communications (ICC) Workshops*, pp. 1129-1133, 9-13 June 2013.
[22] H. Li, X. Xu, D. Hu, X. Tao, P. Zhang, S. Ci, and H. Tang, "Clustering strategy based on graph method and power control for frequency resource management in femtocell and macrocell overlaid system," *J. Commun. Netw.*, vol. 13, no. 6, pp. 664-677, 2011.
[23] H. Dan, L. Hong-jia, X. Xiao-dong, T. Xiao-feng, "Inter-femtocell interference coordination in 3D in-building scenario," *J. China Uni. Posts & Telecomm.,* vol. 19, no. 2, pp. 36-42, 2012.
[24] J. Chen, P. Wang, and J. Zhang, "Adaptive soft frequency reuse scheme for in-building dense femtocell networks," in *Proc. 2012 1st IEEE International Conference on Communications in China (ICCC),* Beijing, 15-17 Aug. 2012, pp. 530-534.
[25] J. Y. Wu, J. Liu, J. Chen, and X. Chu, "Cooperative interference mitigation for indoor dense femtocell networks," in *Proc. 2012 7th International ICST Conference on Communications and Networking in China (CHINACOM),* Kun Ming, 8-10 Aug. 2012, pp. 93-98.
[26] R. K. Saha and C. Aswakul, "A tractable analytical model for interference characterization and minimum distance enforcement to reuse resources in three-dimensional in-building dense small cell networks," *Int. J. Commun. Syst.,* (early view) pp. e3240, 2017, doi: 10.1002/dac.3240
[27] 3GPP, "Simulation assumptions and parameters for FDD HeNB RF requirements," 3rd Generation Partnership Project (3GPP) TSG RAN WG4 (Radio) Meeting #51, R4-092042, May 2009.
[28] A. Tukmanov, Z. Ding, S. Boussakta, and A. Jamalipour, "On the impact of network geometric models on multicell cooperative communication systems," *IEEE Wireless Commun.*, vol. 20, no. 1, pp. 75-81. Feb. 2013.
[29] 3GPP, "Simulation assumptions and parameters for FDD HeNB RF requirements," 3rd Generation Partnership Project (3GPP) TSG RAN WG4 (Radio) Meeting #50bis, R4-091422, Mar. 2009.
[30] 3GPP, "Technical specification group radio access network; evolved universal terrestrial radio access (E-UTRA); FDD home eNodeB (HeNB) radio frequency (RF) requirements analysis (release 9)," 3rd Generation Partnership Project (3GPP), TR 36.921, ver. 2.0.0, Mar. 2010.
[31] J. Ellenbeck, J. Schmidt, U. Korger, and C. Hartmann, "A concept for efficient system-level simulations of OFDMA systems with proportional fair fast scheduling," in *Proc. 2009 IEEE GLOBECOM Workshops*, 30 Nov.-4 Dec. 2009, pp. 1-6.
[32] X. Ge, H. Cheng, M. Guizani, and T. Han, "5G wireless backhaul networks: challenges and research advances", *IEEE Netw.,* vol. 28, no. 6, pp. 6-11, Nov./Dec. 2014.
[33] B. Badic, T. O'Farrrell, P. Losket, and J. He, "Energy efficient radio access architectures for green radio: large versus small cell size deployment," in *Proc. 2009 IEEE 70th Vehicular Technology Conference (VTC 2009-Fall)*, 20-23 Sep. 2009, pp. 1-5.
[34] EARTH, "EU funded research project INFSO-ICT-247733," Energy Aware Radio and neTwork tecHnologies (EARTH), ver. 1.0, 31 Dec. 2010.
[35] Y. Wang, K. I. Pedersen, T. B. Sørensen, and P. E. Mogensen, "Carrier load balancing and packet scheduling for multi-carrier systems," *IEEE Trans. Wireless Commun.,* vol. 9, no. 5, pp. 1780-1789, 2010.
[36] H. J. Bang, T. Ekman, and D. Gesbert, "Channel predictive proportional fair scheduling," *IEEE Trans. Wireless Commun.,* vol. 7, no. 2, pp. 482-487, 2008.
[37] R. K. Saha, "Modified proportional fair scheduling for resource reuse and interference coordination in two-tier LTE-advanced systems," *Int. J. Digital Info. & Wireless Commun. (IJDIWC)*, vol. 3, no. 2, pp. 9-28, 2013.
[38] R. K. Saha and C. Aswakul, "Microwave and millimeter-wave enabled small cell for non-uniform and asymmetric traffic in 5G mobile network," in *Proc. 2017 International Conference on Electronics, Information, and communication (ICEIC),* (to appear in IEEE Xplore), Phuket, Thailand, 11-14 Jan. 2017, pp. 240-243.
[39] 3GPP, "E-UTRA; radio frequency (RF) system scenarios," 3rd Generation Partnership Project (3GPP) TR 36.942, ver. 1.2.0, Jul. 2007.
[40] S. Geng, J. Kivinen, X. Zhao, and P. Vainikainen, "Millimeter-wave propagation channel characterization for short-range wireless communications," *IEEE Trans. Veh. Technol.,* vol. 58, no. 1,

pp. 3-13, Jan. 2009.
[41] T. Yilmaz, E. Fadel, and O. B. Akan, "Employing 60 GHz ISM band for 5G wireless communications," in *Proc. 2014 IEEE International Black Sea Conference on Communications and Networking (BlackSeaCom)*, 27-30 May 2014, pp. 77-82.
[42] D. L. Pérez, M. Ding, H. Claussen, and A. H. Jafari, "Towards 1 Gbps/UE in cellular systems: Understanding ultra-dense small cell deployments," *IEEE Communn. Surveys & Tuts.*, vol. 17, no. 4, pp. 2078-2101, 2015.
[43] R. K. Saha, P. Saengudomlert, and C. Aswakul, "Evolution toward 5G mobile networks—A survey on enabling technologies," *Engineering Journal*, vol. 20, no. 1, pp. 87-119, 2016.